

SiPM: features and applications

Giulio Saracino
University of Naples
Federico II

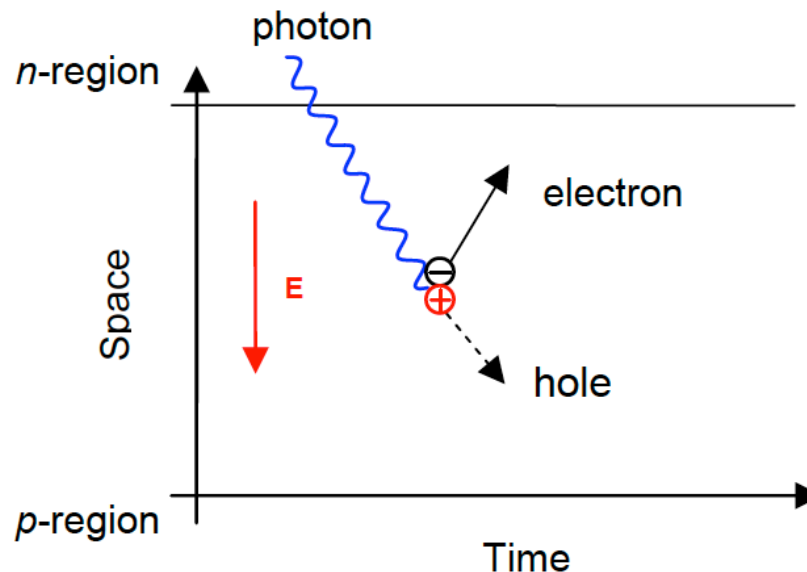
OUTLINE

- Introduction to Si photon detectors
- SiPM features
- Applications
- Conclusions

Photon absorption in Si (I)

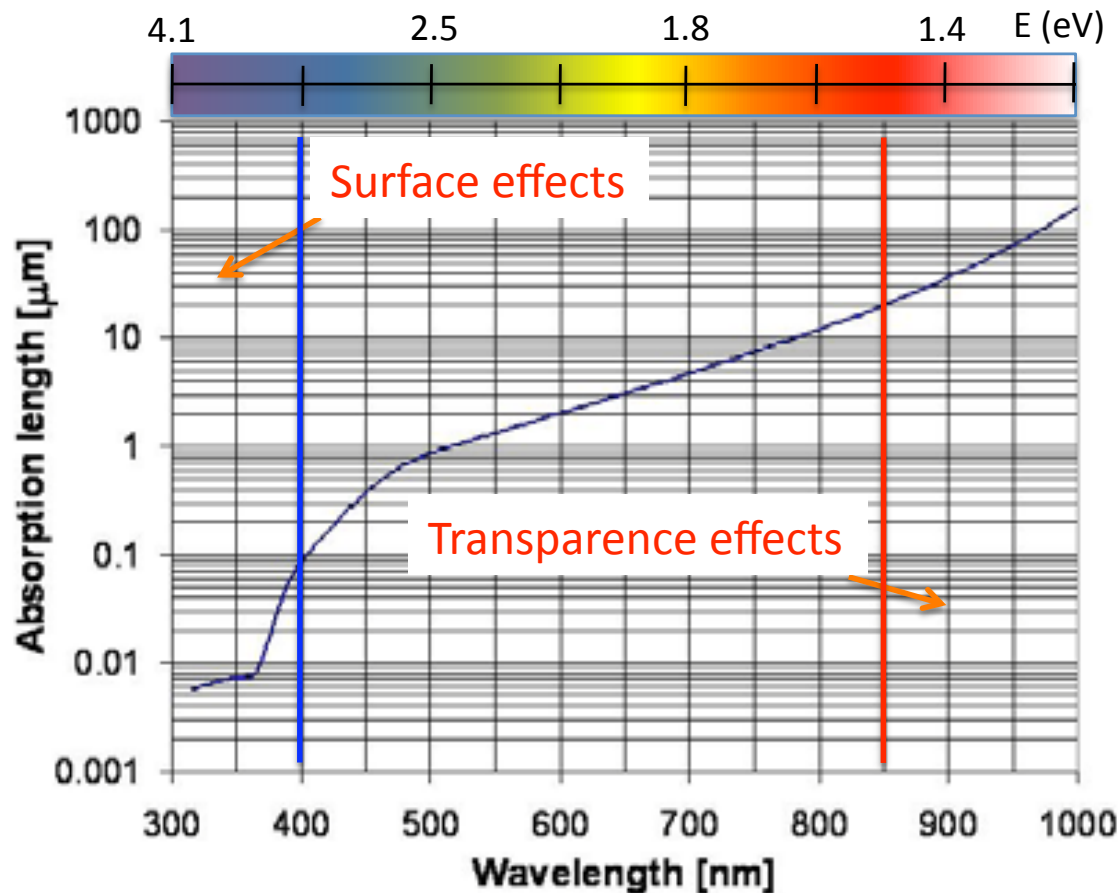
Photon with energy higher than band gap (1.1 eV for Si) can be absorbed creating electron-hole pairs that drift by effect of the applied electric field, inducing a signal through the external electric circuit.

Typically the sensitive volume is the depleted region of a N-P junction biased in reversed mode.



Photon absorption in Si (II)

Photon flux at a distance d from the surface: $I(d) = I(0)e^{-d/D}$



Absorption length D in visible region:

- depends strongly on the WL
- dominated by **photo-electric effect**

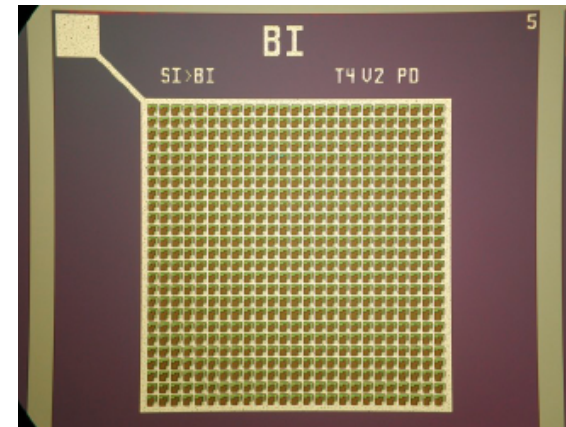
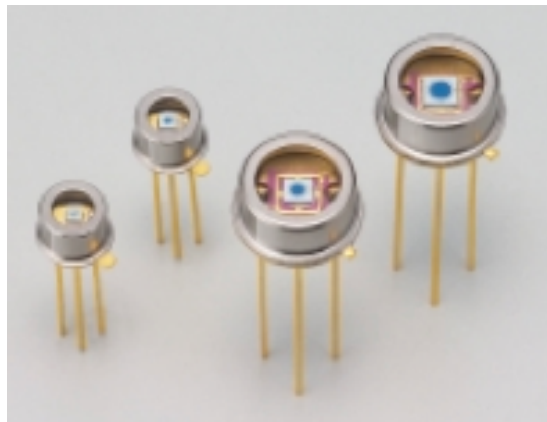
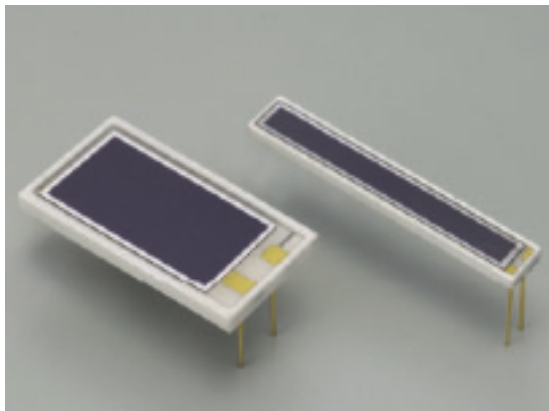
$\lambda < 400$ nm: photons are absorbed into the passivation layer before they reach the sensitive zone

$\lambda > 850$ nm: photons are (not) absorbed after the sensitive zone

Si photo-detectors

Three main typology :

type	Internal gain	Minimal detectable signal (p.e.)	Bandwidth	Max Size
PIN photodiodes	NO	200-300	Few 100 kHz	10 cm ²
APD	Linear 50-200	10-20	MHz-few 100MHz	2.5 cm ²
SiPM	Geiger, $10^5 - 10^6$	1	MHz-few 100MHz	< 1 cm ²



Si APD working principles

PIN photodiodes

signal is given by e-h pairs directly produced: no internal gain.

External amplification needed for small signals. Minimal detectable signal ≈ 200 photons

APD: Internal gain

If the E field is high enough electrons and holes can start an avalanche (impact ionization)

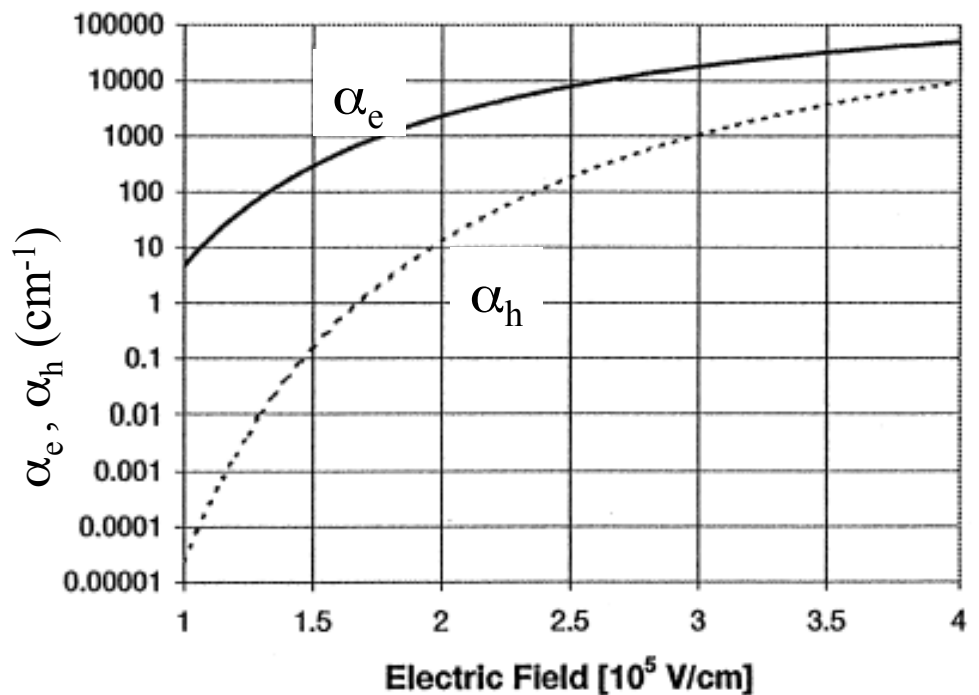
two exponential laws:

$$G_e = e^{\alpha d} \quad \alpha_e = \alpha_0 e^{-E_0/E}$$

h contribution is minor, but crucial!
proportionality if $\alpha_e/\alpha_h \gg 1 \Rightarrow \text{Si}$

When $G_h > 2 \Rightarrow$ Geiger avalanche is started:

- proportionality is loss
- big signal
- quenching needed



APD features

Advantages

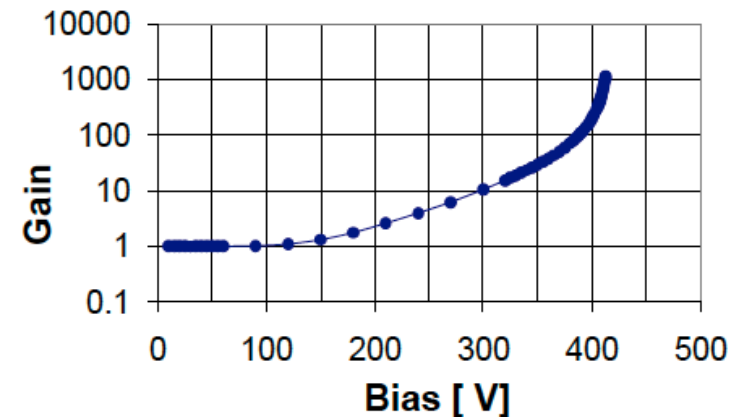
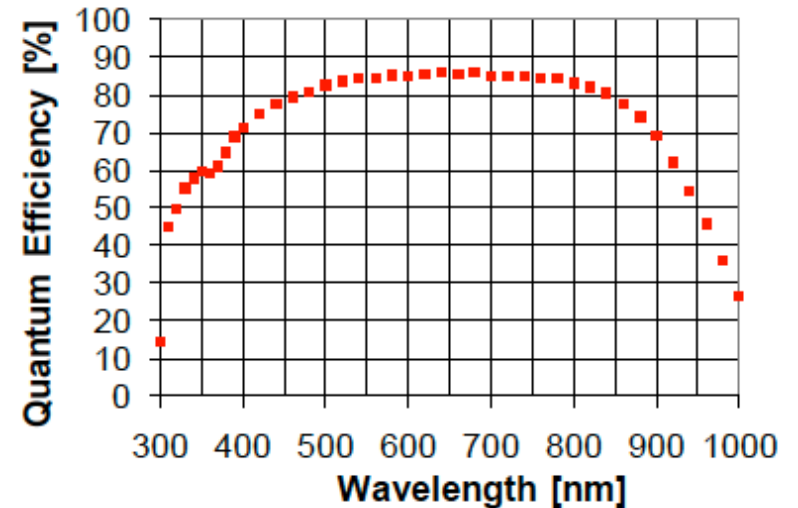
- High QE
- G up to 1000
- Area up to 2 cm² (limited by uniformity in the gain)
- Moderated external amplification needed 10-100

Disadvantages:

- the internal gain is a stochastic process -> excess noise factor introduced.
- Temperature dependence.

The best S/N is achieved when the hole gain contribution is minimum -> reach-through structure.

Single photon sensitivity:
possible but at low temperature and dedicated electronic (VLPC structure used in D0.)



APD in Geiger mode

APD can work in Geiger mode:

- Signal is no more proportional to impinging number of photons
- Gain is high and with no excess noise factor -> single photon sensitivity achievable
- The Geiger discharge is self-sustaining: it must be broken by a quenching external mechanism

Passive quenching: a serial resistor decreases the effective bias during the discharge

- Easy to implement (either by an external resistor or imbedded by semiconductor itself)
- Very long dead time

Active quenching: external circuit that reduce the dead time

This technology was studied since 1960, but no big success achieved:

- No proportionality
- Active area < 1mm² otherwise low temperature required
- Active quenching in order to reach good rate capability



Features

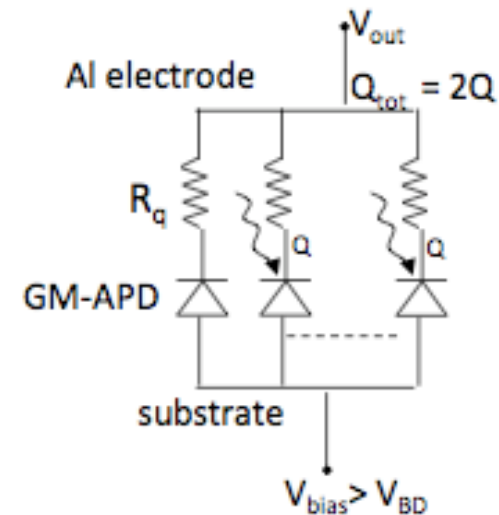
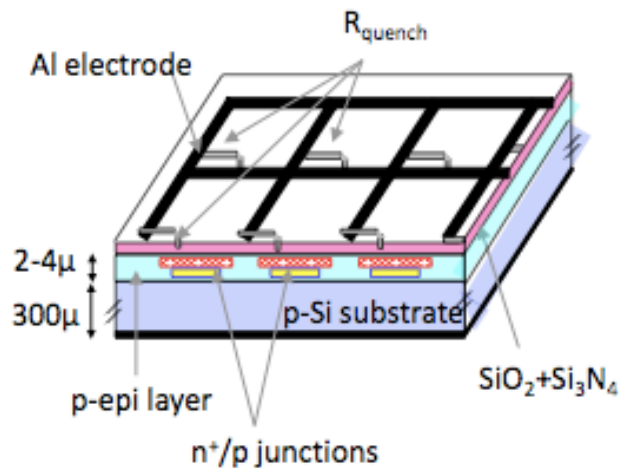
- Peak Photon Detection Efficiency @ 650 nm:
- 70% Typical
- Active Area: SPCM-AQR-1X: 175 μm
- Timing Resolution of 350 ps FWHM
- User Friendly
- Gated Input
- Single +5v Supply

Dark count rate – 500 Hz (25 Hz -selected)

Multi cell G-APD: SiPM

The big improvement comes from a “simple” idea: many small G-APD cells connected in parallel with a common substrate and individual quenching resistors.

The Silicon photon-multiplier was born!



The name “SiPM” reflects the single photon sensitivity capability of classic photo-tubes. Many fathers -> many names : MRS APD, MAPD, SSPM, MPPC, SPM, DAPD, PPD....

SiPM in one slide

Main features:

- high photo-detection efficiency (25%-70%)
- Linearity ($n \text{ photons} \ll n \text{ cells}$)
- High gain (10^5 - 10^6)
- Single photon detection sensitivity
- no excess noise factor (at first order..)
- fast ($\approx 1 \text{ ns}$ rise time)
- good time resolution ($< 100 \text{ ps}$)
- Low bias voltages ($< 100 \text{ V}$)
- Insensitive to B field

Limits: Dark counts, surface area, temperature dependence.

SiPM features

Photon detection efficiency

$$\text{PDE}(\lambda, \Delta V) = \epsilon_{\text{geo}} \cdot \text{QE}(\lambda) \cdot \epsilon_{\text{AT}}(\lambda, \Delta V)$$

$$\Delta V = V_{\text{bias}} - V_{\text{BD}}(T)$$

ϵ_{geo} = geometrical factor: 0.2 ÷ 0.8

$\text{QE}(\lambda)$ = quantum efficiency: close to 1 in the blue-green region

$\epsilon_{\text{AT}}(\lambda, \Delta V)$ = avalanche trigger probability > 0.95 when $\Delta V/V_{\text{bias}} > 0.15$

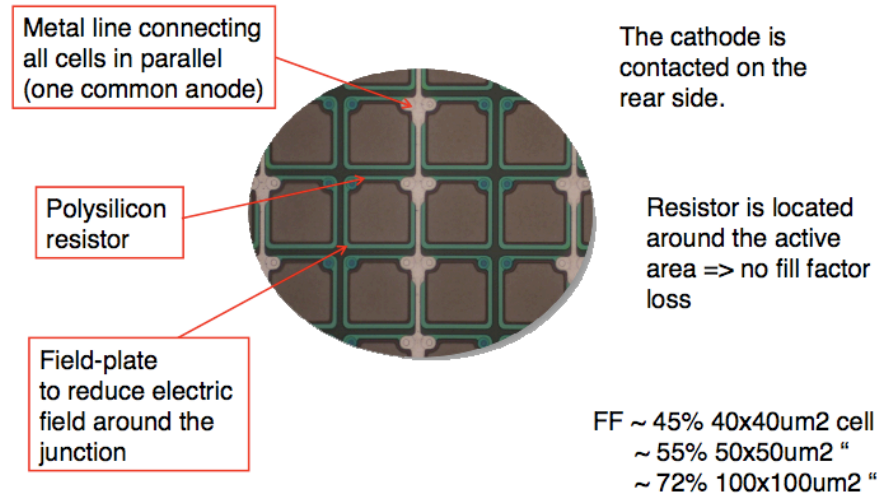
$$\epsilon_{\text{geo}}$$

Geometric efficiency = Sensitive area/ total area

Metal lines connecting the cells, poly-silicon resistor, trenches and implantation profile reduce the sensitive area

Fill factor increases with increasing cell size,
can reach 70-80 %

Producer	SiPM ID	No. μ cells	μ cell size (μm)	ϵ_{geom} (%)
Photoniq	SSPM-0701-BG	556	43×43	70
FBK-irst	W20-B10-T3V2PD/I run	625	40×40	20
FBK-irst	W3-B3-T6V1PD/II run	625	40×40	16
SensL	SPM-20	848	29×32	43
SensL	SPM-35	400	44×47	59
SensL	SPM-50	216	59×62	68
HPK	S10362-11-25	1600	25×25	31
HPK	S10362-11-50	400	50×50	61.6
HPK	S10362-11-100	100	100×100	78.5



C. Piemonte

IPRD10, Siena, 8 June 2010

5

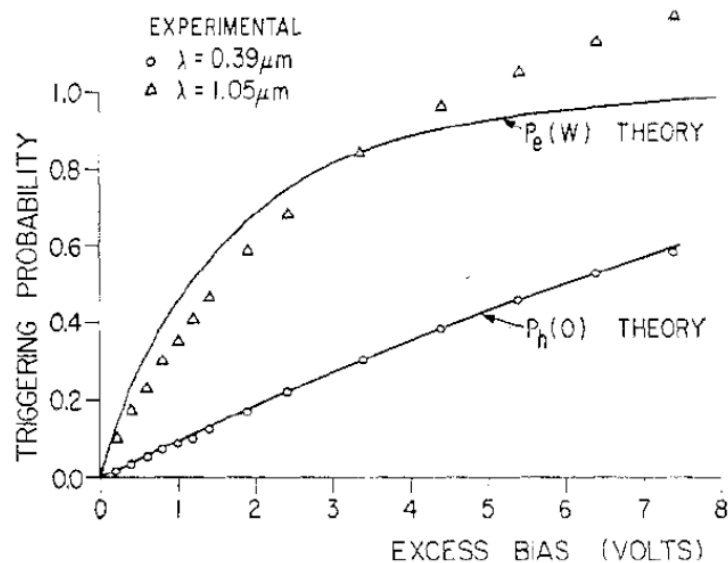
Trigger probability

Geiger discharge can be triggered by electrons or by holes.

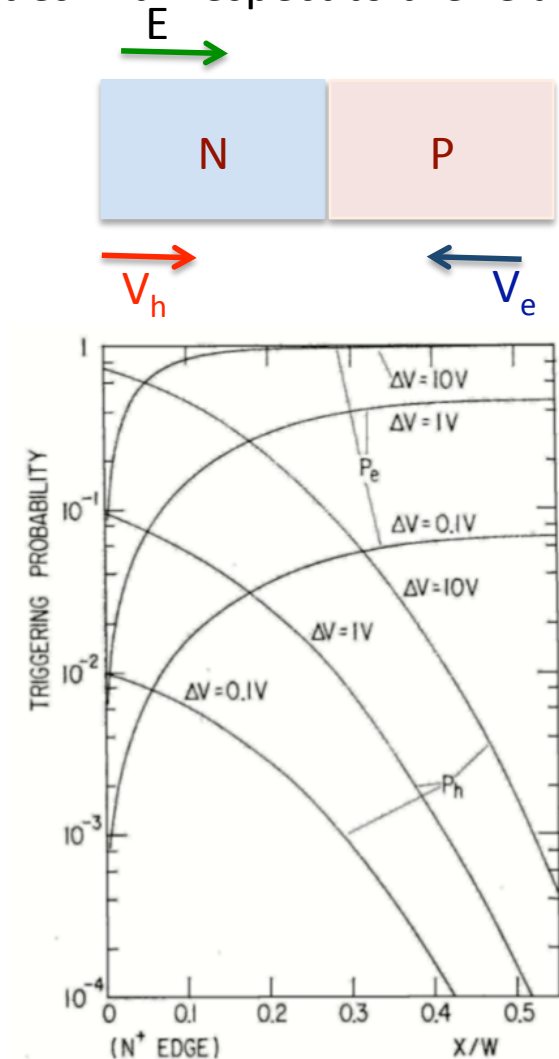
For a certain E field the hole trigger probability is lower than for electrons.

The final probability will be obtained by integrating the probabilities with respect to the relative distance X/W traveled by the carriers.

Conversion in the P region gives better chance to start an avalanche because e can travel the full depletion length W !!

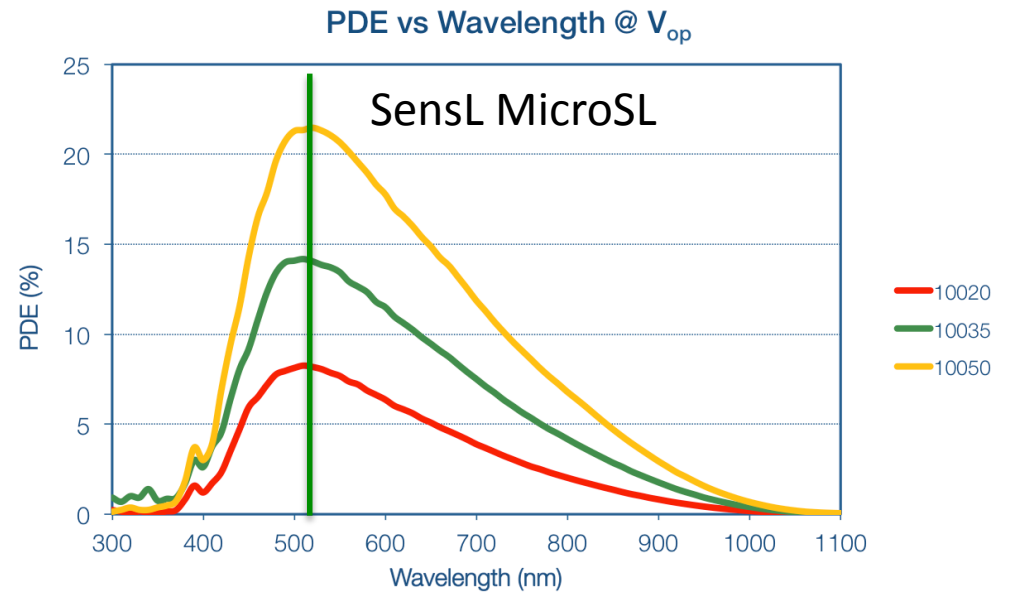
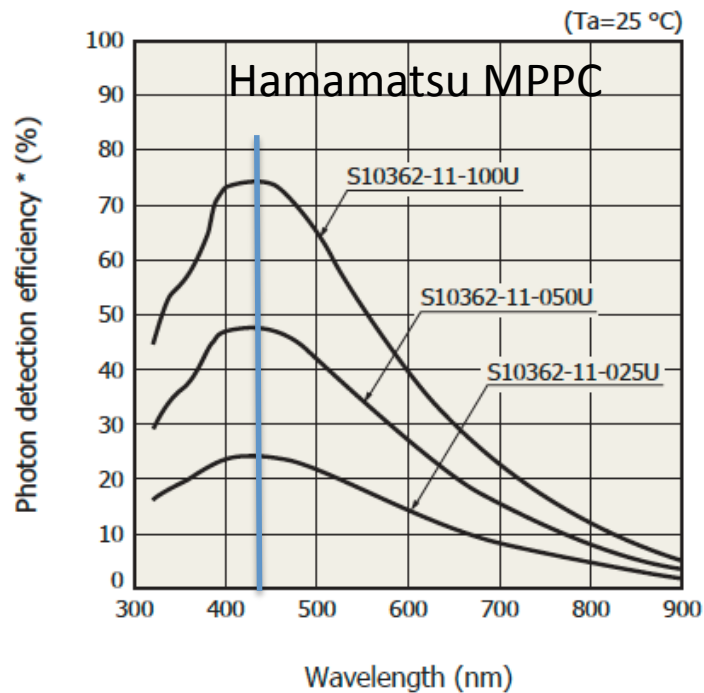
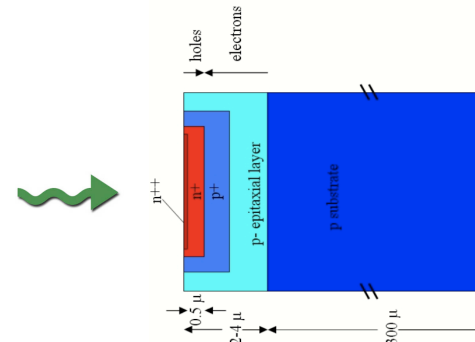
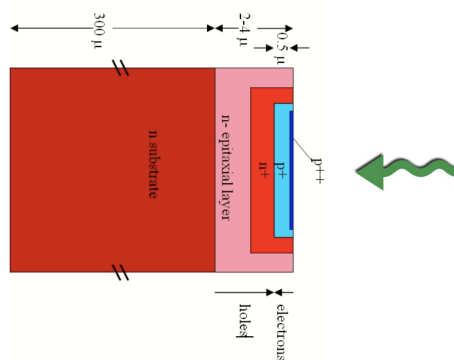


W.G. Oldhan et al. IEEE transactions on electronic devices, Vol. 19 1972



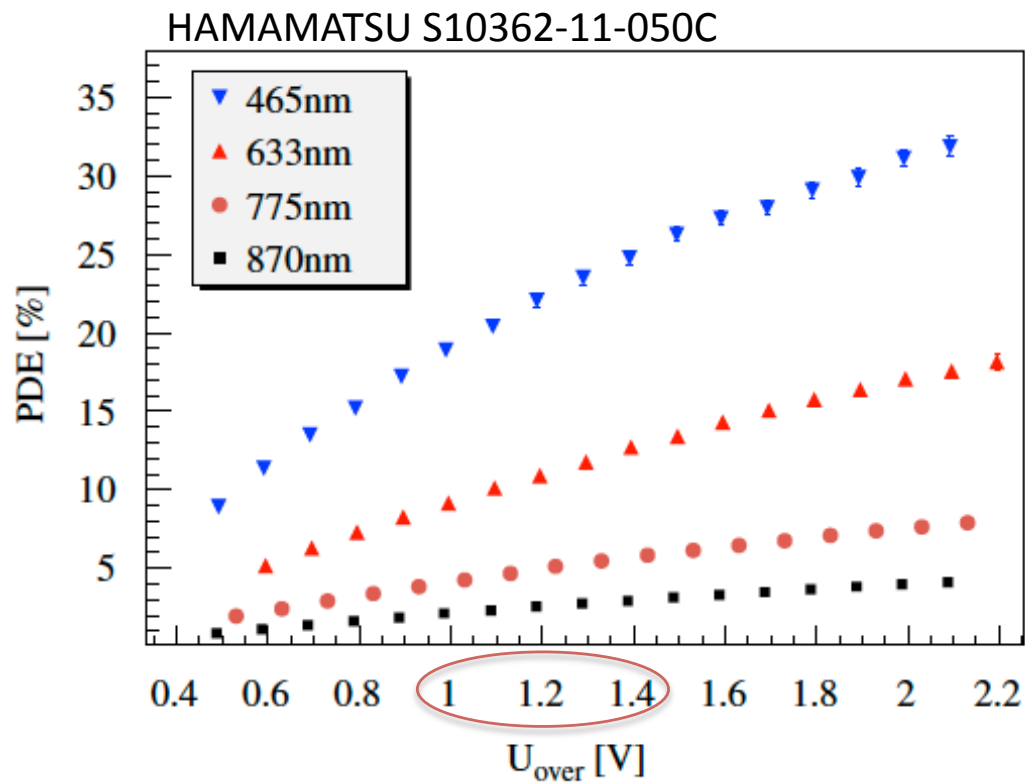
PDE(λ) curves

Depending of the type of technology the maximum is reached in the blue (PON) or green (NOP) region



PDE(V_{bias}) curves

Typical operating voltages are not in the trigger efficiency saturation region



P. Eckert et al. / Nuclear Instruments and
Methods in Physics Research A 620
(2010) 217–226

Note on PDE measurement

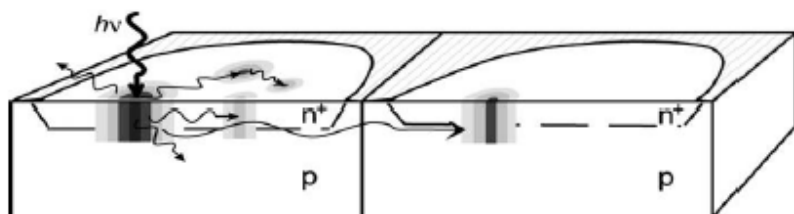
Recently several authors have noticed that PDE measurement are often overestimated due to two undesired effects:

- Optical cross talk
- After pulsing

which also introduce an excess noise factor !

Optical cross talk

During the avalanche photons can be produced crossing cell and starting a new avalanche

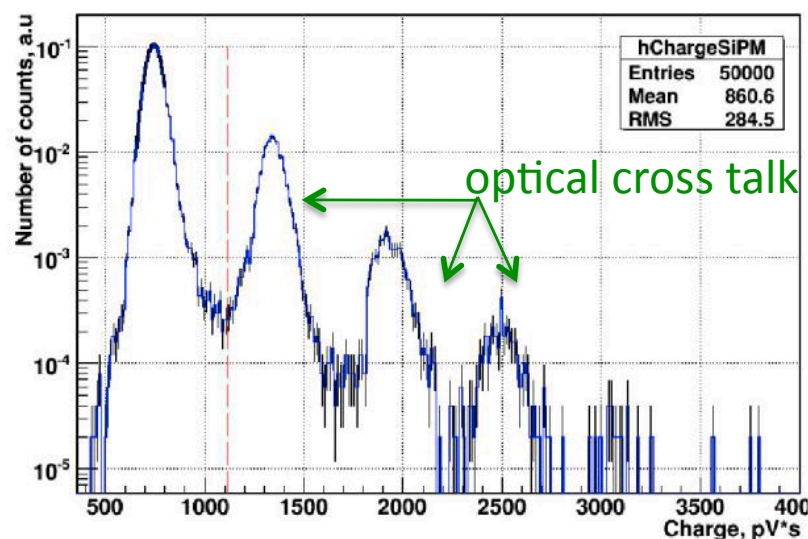


10^5 carriers produce ~ 3 photons with wavelength less than $1 \mu\text{m}$

process is very fast: on time signals



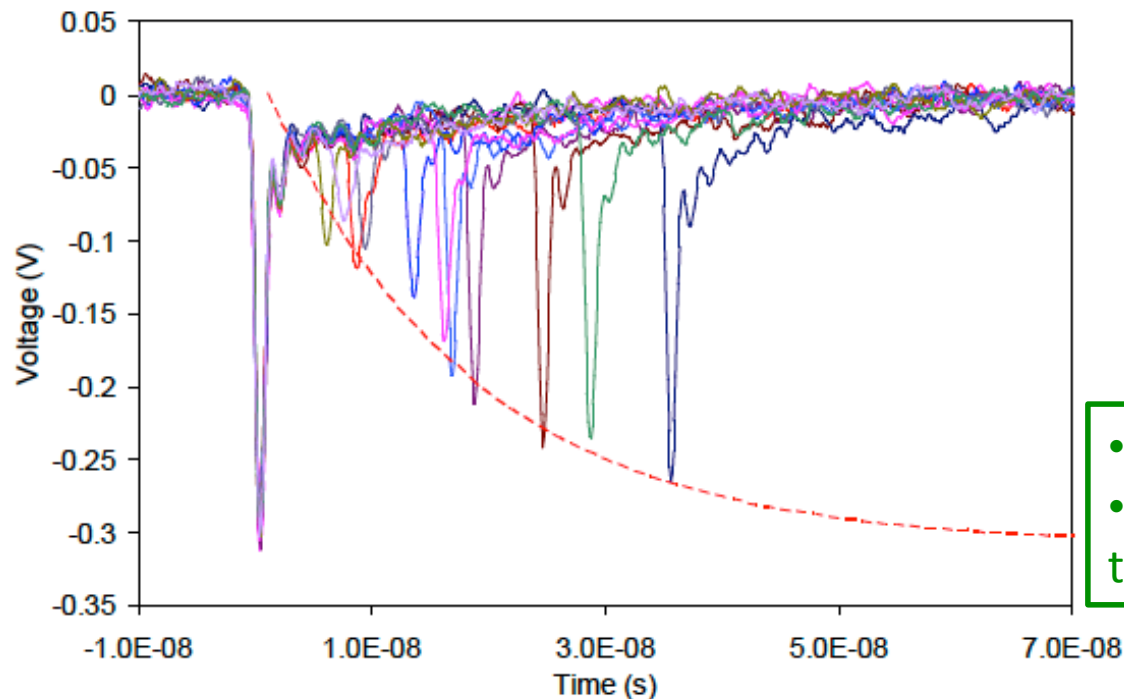
Dark noise spectrum



After-pulsing

Once a cell has fired there is a probability that it fires again, due to the trapping and releasing of carriers

Since the cell requires some time to recharge after breakdown, after-pulse amplitude depends on the time

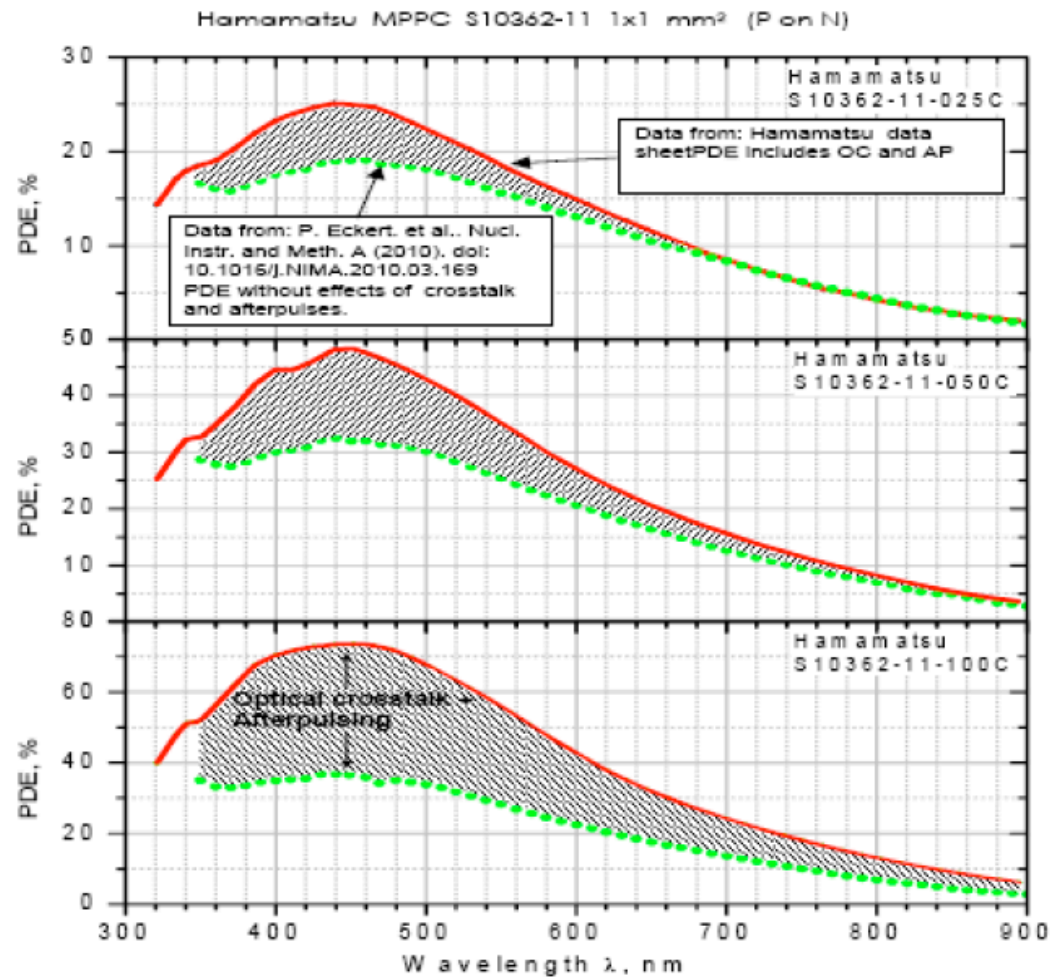


- characteristic time $\tau \approx 100$ ns
- probability is a quadratic function of the overvoltage

(C. Piemonte: June 13th, 2007, Perugia)

PDE Measurement

The red line is the claimed PDE. The green one is measured (Eckert et al.)



Difference comes from the optical cross talk and afterpulsing contribution !
Increase with the pixel size

P. Eckert et al. / Nuclear Instruments and Methods in Physics Research A 620 (2010) 217–226

R. Mirzoyan, Light-11, Rinberg, Germany

7/3/12

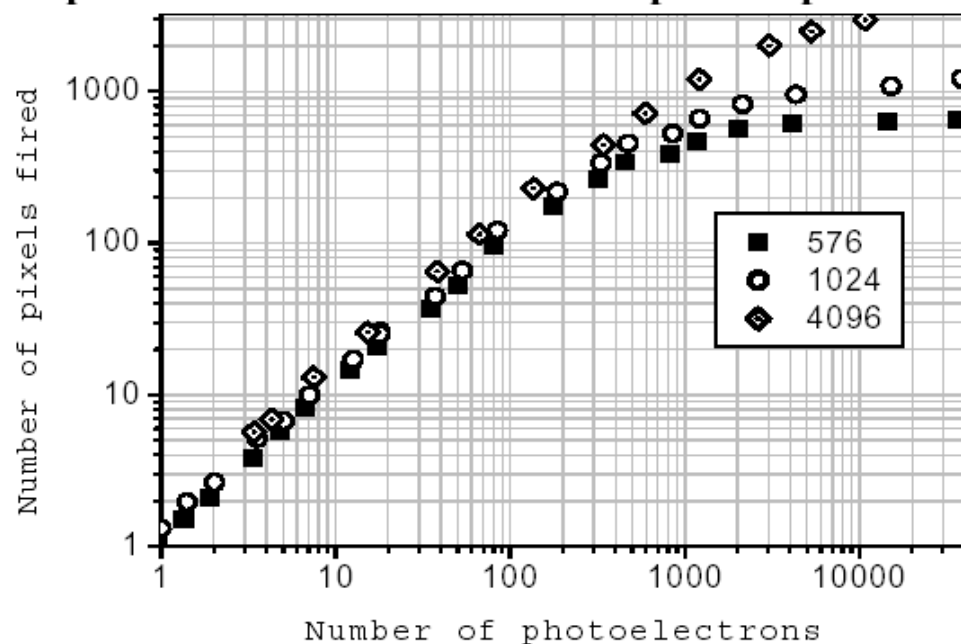
G. Saracino

20

SiPM linearity

The single cell is “digital”: the amplitude is independent on the number of photons.
Linearity is obtained by summing signals from different cells

Response functions for the SiPMs with different total pixel numbers measured for 40 ps laser pulses



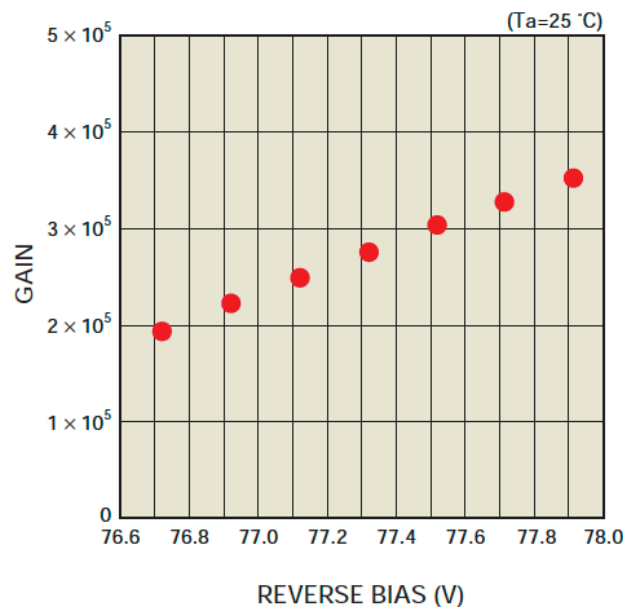
- Linearity is true for $N_\gamma \ll N_{\text{cell}}$
- Increasing the number of cell increases the linearity range

V. Andreev et. al., Nucl. Instrum. Meth. A 540 (2005) 368.

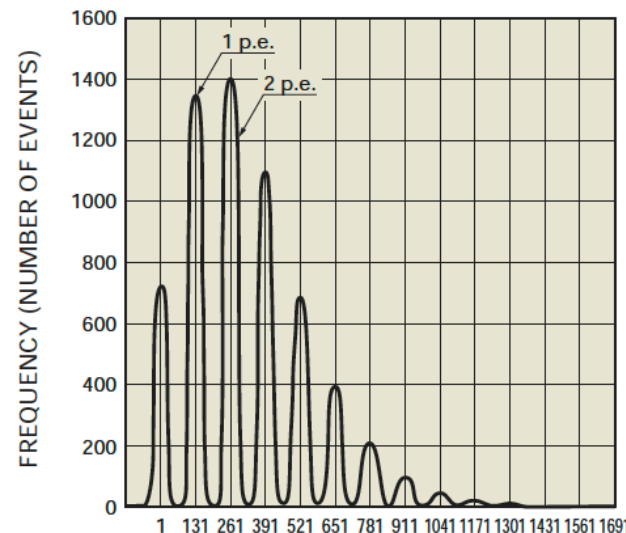
Gain (I)

In ideal SiPM the charge Q released by the avalanche is due to cell capacitance discharge:

$$Q = C(V_{\text{bias}} - V_{\text{bd}}) \rightarrow G = Q/q_e$$



It is linear with respect to the bias voltage.



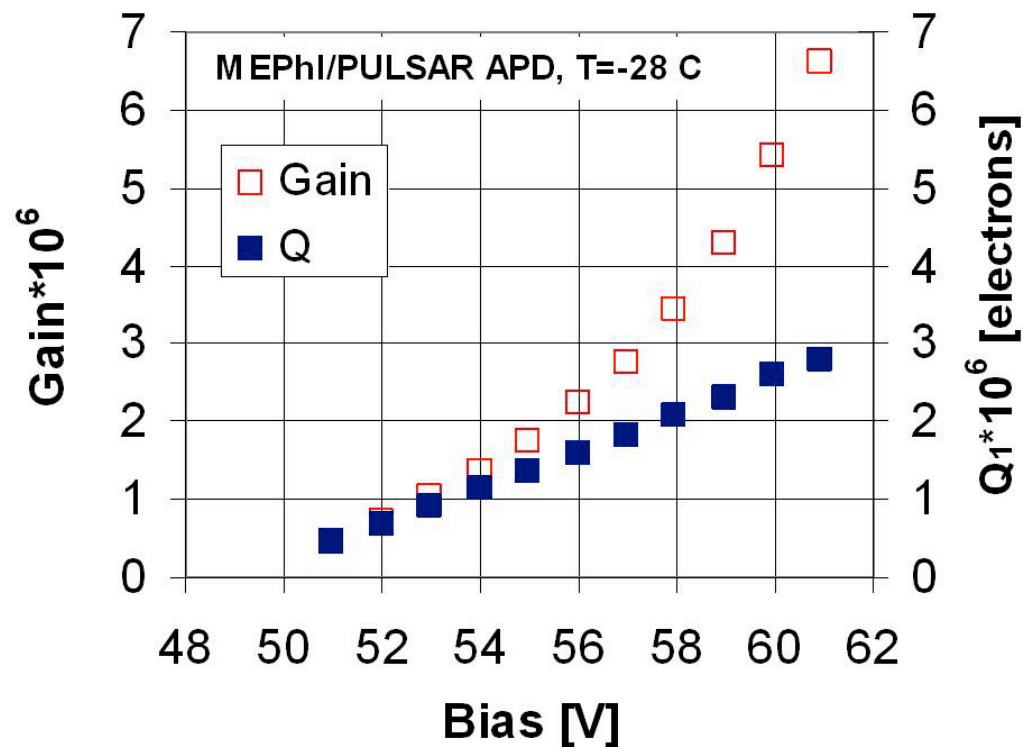
Hamamatsu
datasheet

very good pixel-pixel uniformity of the gain

Gain can be measured by the charge spectrum
(generated by dark counts or by low intensity light sources)

Gain (II)

The effect of cross-talk and after-pulsing introduce non linearity and an excess noise factor.



$$G = \langle N_{\text{pix}} \rangle \times Q_1$$

Musienko et al.: NIMA 567 (2006) 57–61

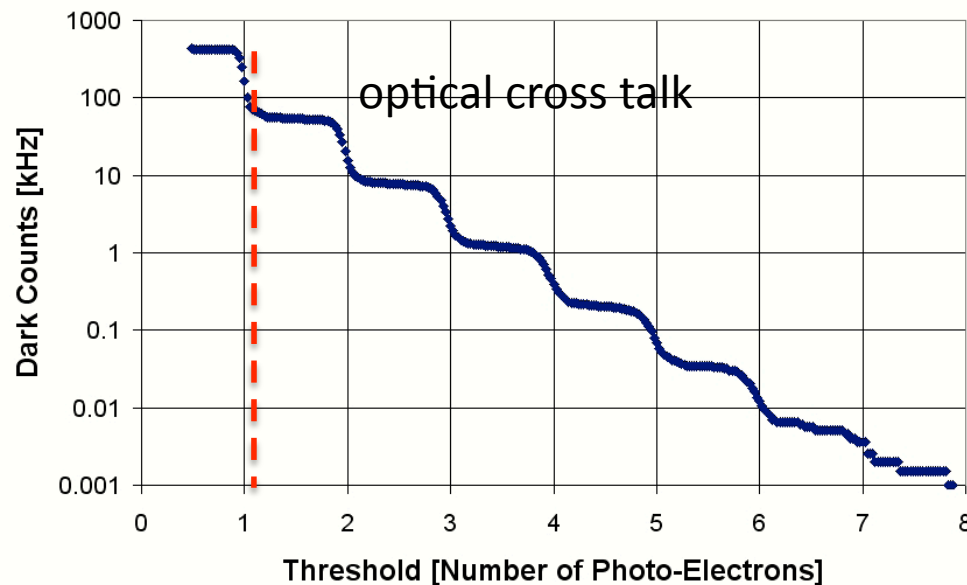
Dark counts

Still in absence of light we can observe signals called dark current or dark counts.

Free carriers can be produced mainly in two ways

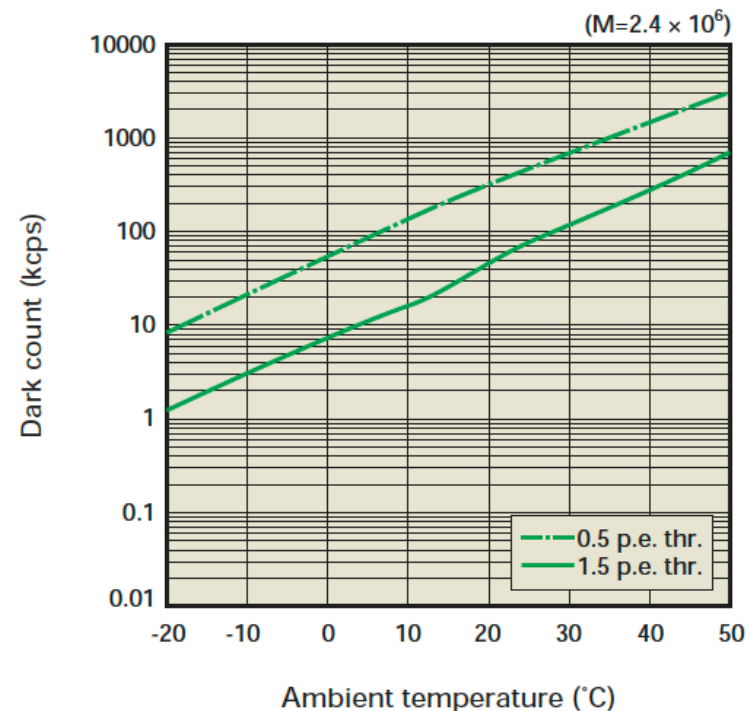
- thermally: they can be reduced by cooling (factor ≈ 2 reduction every 8°C drop)
- field assisted generation: lower than therm. but can be reduced only by reducing the E field

typical ranges are 100 kHz to several MHz per mm^2 at 25°C



rates can be reduced by one order of magnitude increasing thresholds of one photoelectron equivalent

(c) S10362-11-100U/C



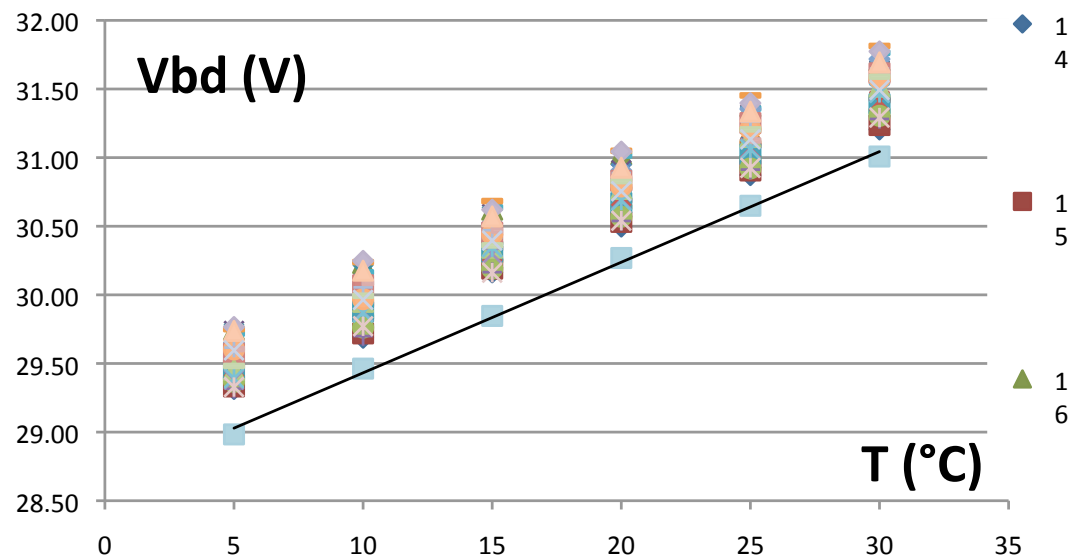
Temperature dependences

SiPM can work fine at room temperature but they are sensitive to temperature changes!

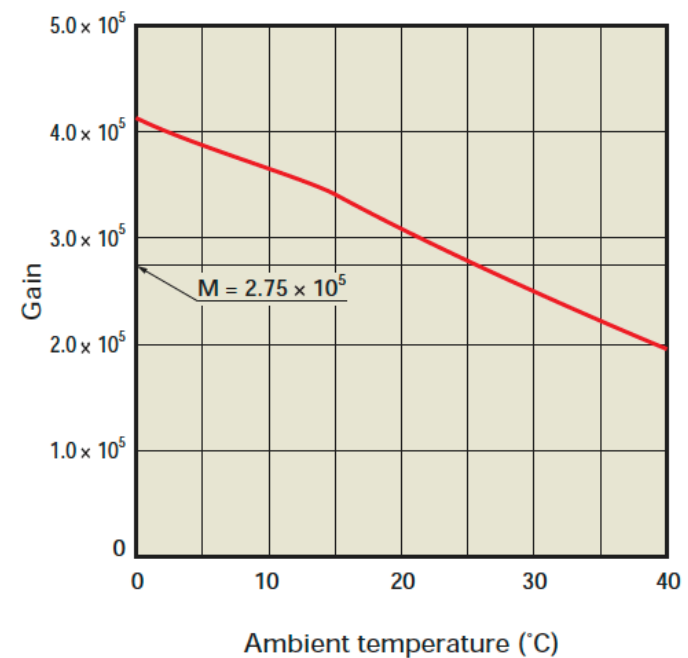
The main issue is the change of V_{bd} . if V_{bias} is not changed, the change in temperature leads to change in gain and PDE.

$$dA/dT * 1/A \approx 0.3\%/^{\circ}\text{C}$$

Hamamatsu S10362-11-025U/C



$$\text{IRST } dV_{BD}/dT = 80 \text{ MV}/^{\circ}\text{C} = 0.23 \text{ } \%/^{\circ}\text{C}$$

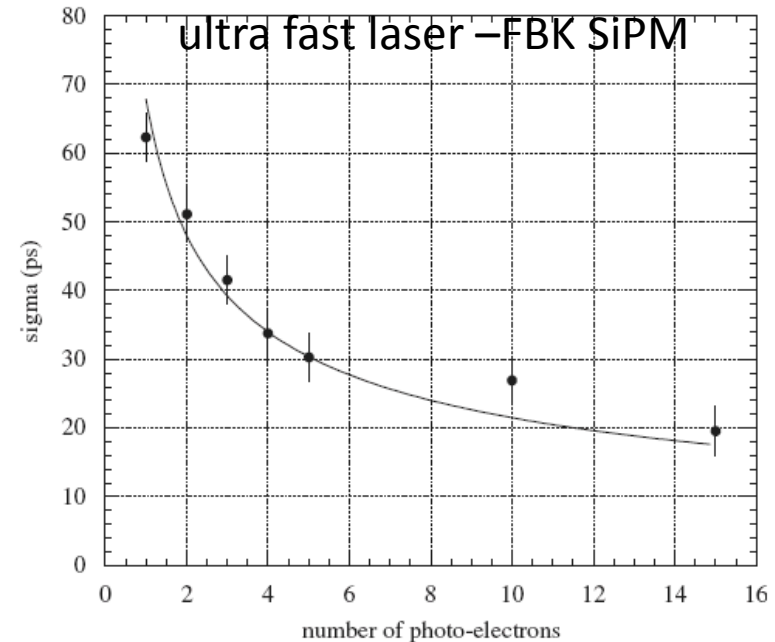
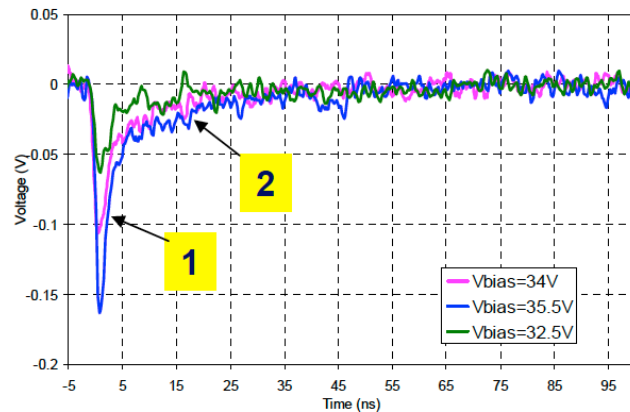


Gain change at fixed V_{Bias}

Timing properties

Active layer is very thin (2 – 4 μm) and breakdown process is fast. Charge released is big:
good timing properties even for single photo-electron!

Rise time is determined by resistance of silicon in the breakdown channel, space charge, resistance of the neutral regions, parasitic capacitance of the whole device ($\sim 10 \text{ pF} \gg \sim 100 \text{ fF}$ of single cell)



G. Collazuol et al./ NIMA 581 2007 461-464

Recovery time depends by the quenching resistor and cell capacitance: $t = RC = 5 - 100 \text{ ns}$
some devices (FBK) show two components

SiPM applications

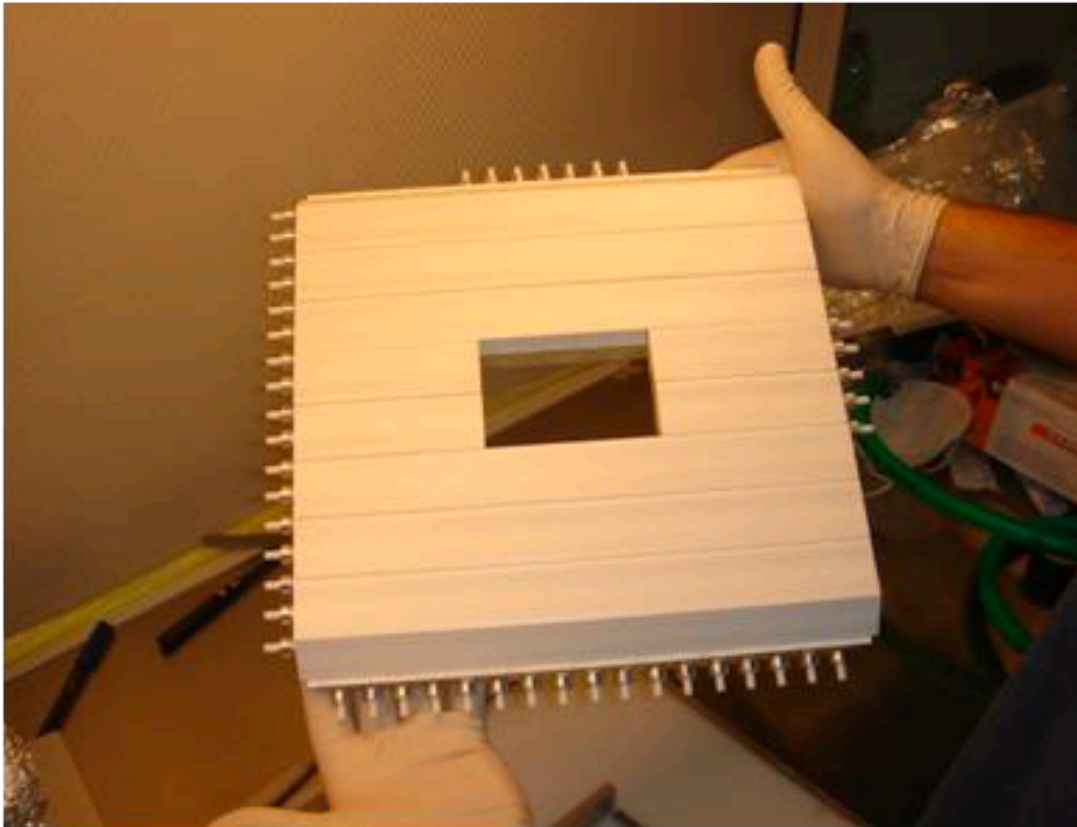
HEP

- T2K Near Detector: 64.000 (POD, FGDs, ECal, SMRD, INGRID)
- CMS 3000 (HO HCAL)
- ILC: 8000 CALICE hadron calorimeter
- FACT: 1500 (First gApd Cherenkov Telescope)
- MICE proposed for the electron-muon calorimeter
- NA62: 300: Charged Anti-counter

No HEP:

- PET
- Intra-operative Beta Probes
- Muon Radiography MU-RAY

The NA62 CHarged ANTICounter



CHANTI

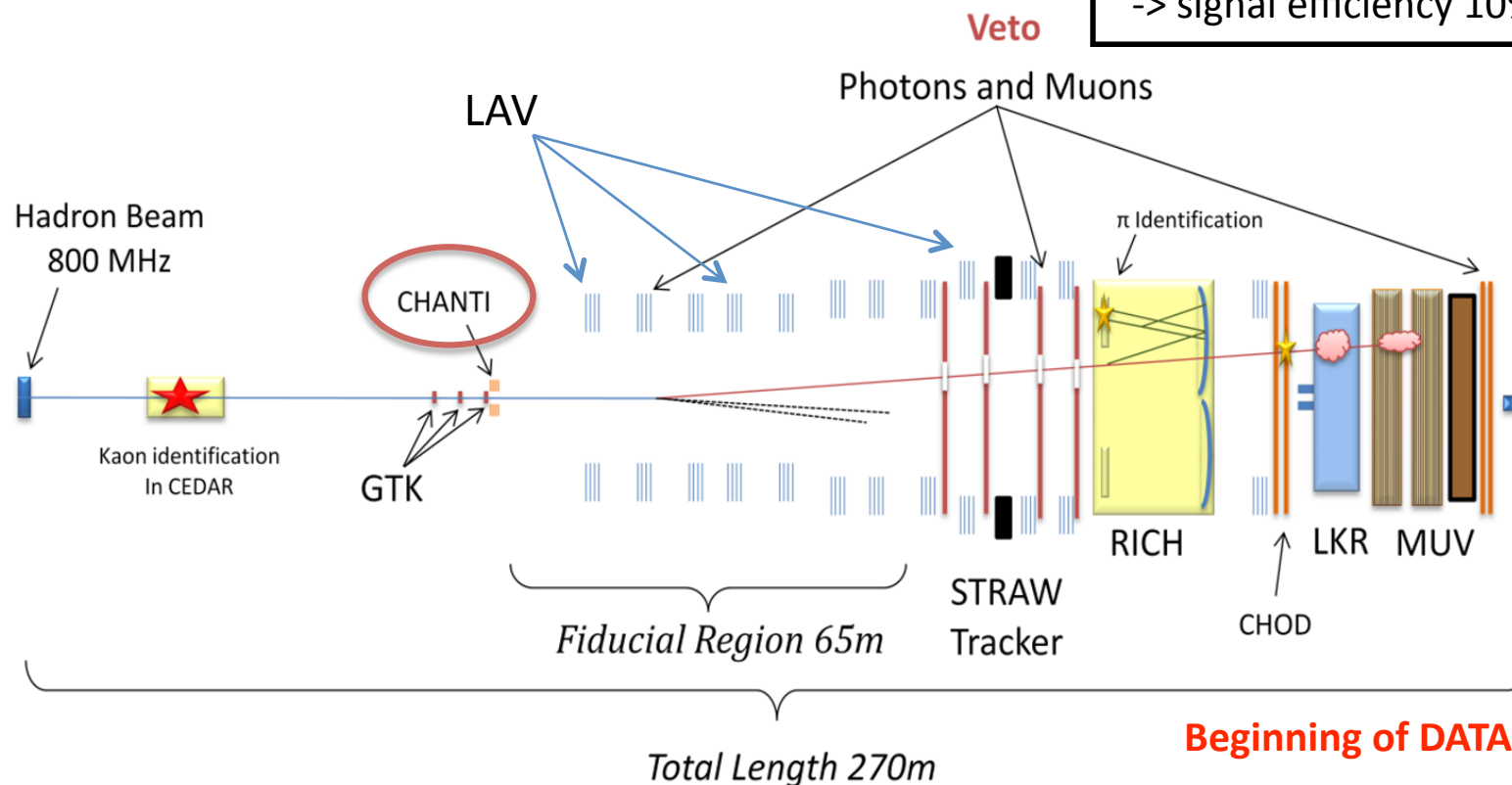
The NA62 experiment (CERN)

Measure the $K^+ \rightarrow \pi^+ \nu \bar{\nu}$ B.R. with high accuracy

- Expected B.R. $(8.5 \pm 0.7) \times 10^{-11}$
- Goal: to collect ~ 100 decays with $S/B \sim 10$ (two years)

Unseparated Beam:

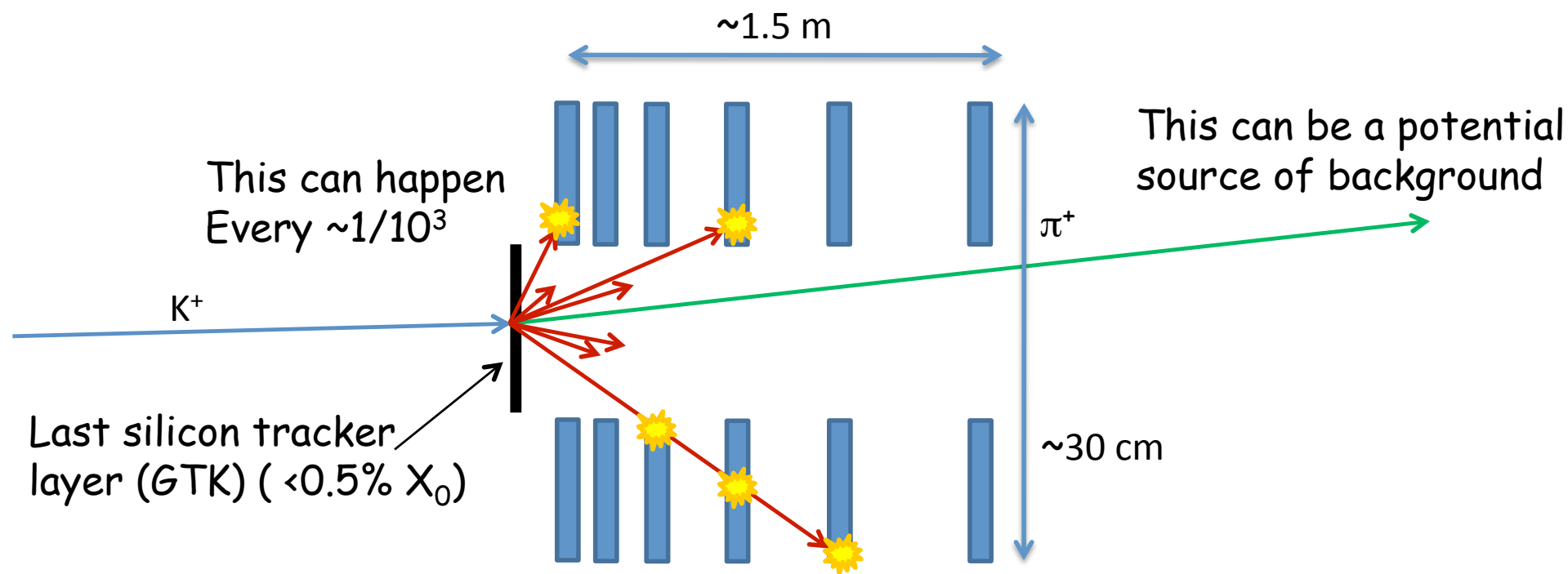
- > Momentum 75 GeV/c
- > Kaon beam percentage $\sim 6\%$
- > # Kaons decays $4.8 \times 10^{12}/\text{yr}$ (40 MHz)
- > signal efficiency 10%



Beginning of DATA TAKING: 2014

CHANTI purpose

To reduce background induced by beam inelastic interaction with beam tracker



Inelastic interactions can be identified detecting the large angle products using a set of six "guard rings"

95% of inelastic interactions can be detected by CHANTI.

REQUIREMENTS

- Good time resolution (1ns)
- Good rate capability (up to some tens kHz/cm²)
- Low out-gassing (vacuum)
- X-Y coordinate (for timing correction)

Note: the 6 counters can be used as tracker, with few mm spatial resolution, to monitor beam halo muons close to the beam

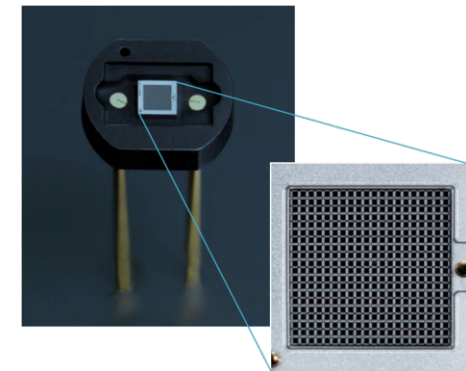
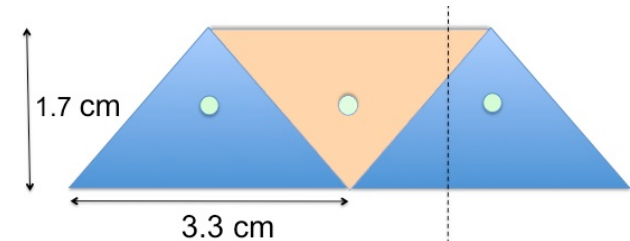
Technological choice

Scintillator bars with WLS fibers read by Si Photomultiplier

- Scintillators: triangular shape for a gap-free and self-sustaining structure (produced by FERMI-LAB for MINERVA, and T2K POD)
- Improve space resolution
- WLS fibers: allow the SiPM-scintillator coupling with excellent optical properties

WLS fiber: BCF92 multi-clad: fast emission time (2.7 ns) mirrored at one side.

SiPM low power consumption -> fine to operate in vacuum

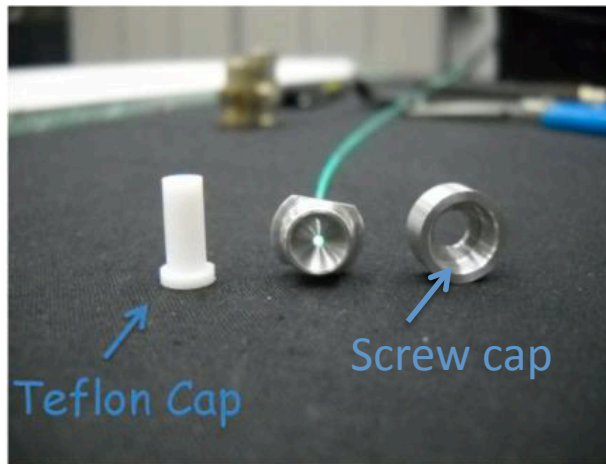


Hamamatsu MPPC S10362 13-50C

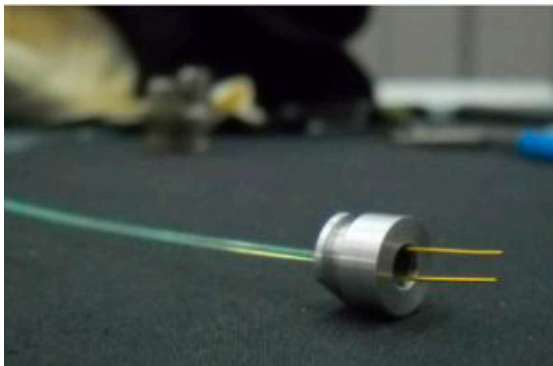
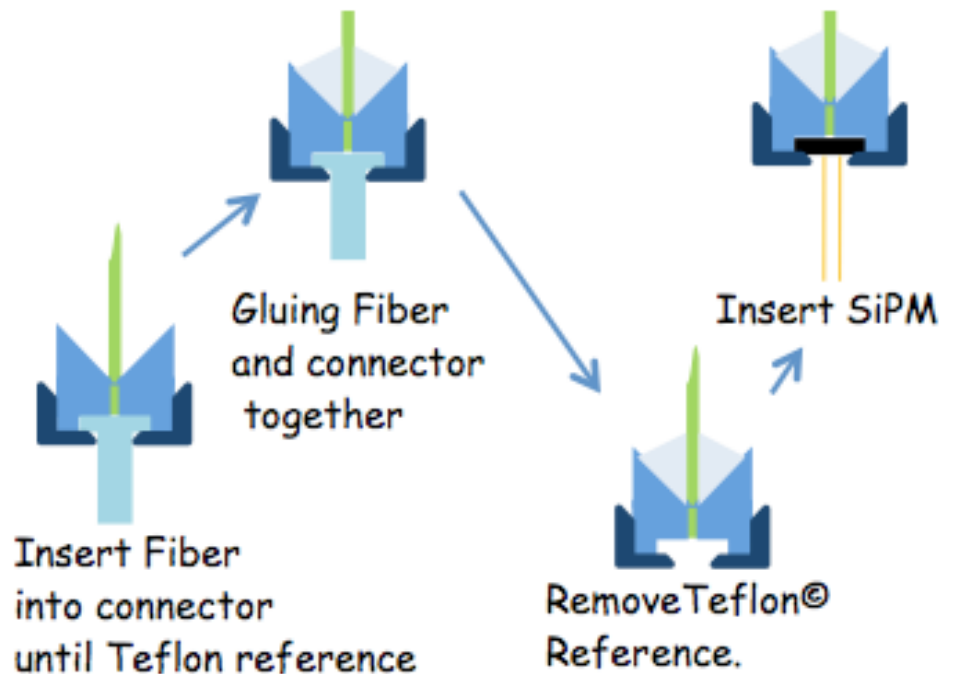
- 1.3 mm side
- 50 μm cell side
- Fill factor 61.5 %
- #cells: 676

Prototype : the fiber-SiPM connector

A custom connector has been designed



A Teflon cap define the reference plane for the fiber
It used to protect the polished side of the fiber
during transport and handling.
Fiber is glued using a small amount of ARALDITE 2011



Fiber-SiPM coupling is:

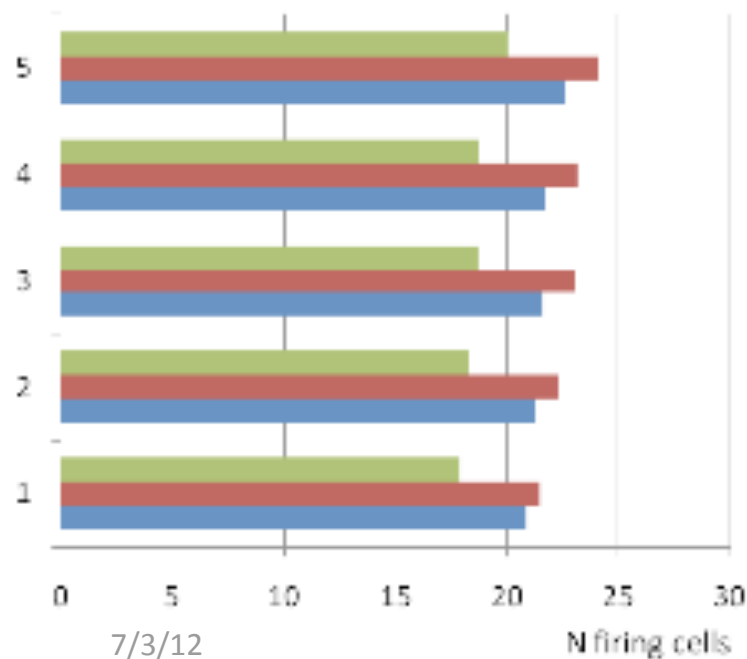
- precise at $50\text{ }\mu\text{m}$ level
- reproducible

SiPM model selection

Three different Hamamatsu MPPC were tested. The number of photoelectron of 5 SiPM of each type was measured using a Sr^{90} source as reference, at the V_{op} bias voltage

MPPC	Side size (mm)	Cell size (μm)	#cells	Fill factor(%)
13-50	1.3	50	676	61.5
11-50	1	50	400	61.5
11-100	1	100	100	78.5

The 13-50 type has the greatest PeY



■ SiPM 11_50 Serie
■ SiPM 13_50 serie
■ SiPM 11_100 seri

distance to photosensitive surface:
 200 μm air + 300 μm silicone resin
 $\approx 150 \mu\text{m}$ max displacement

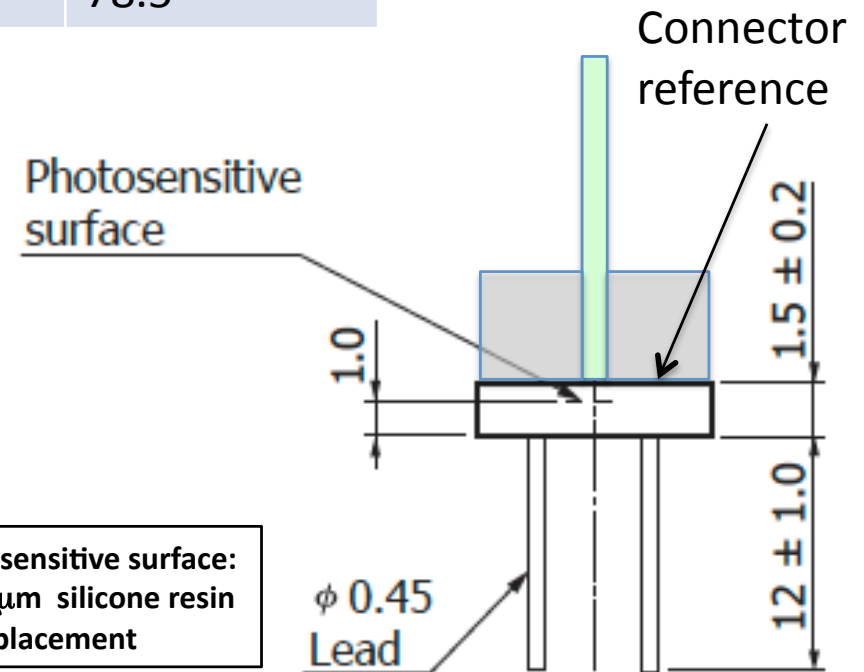
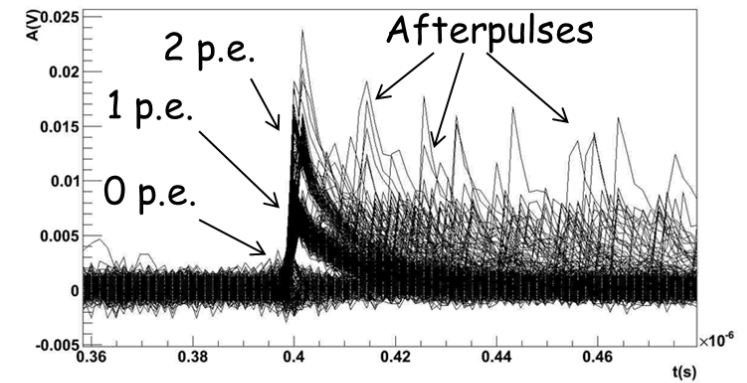
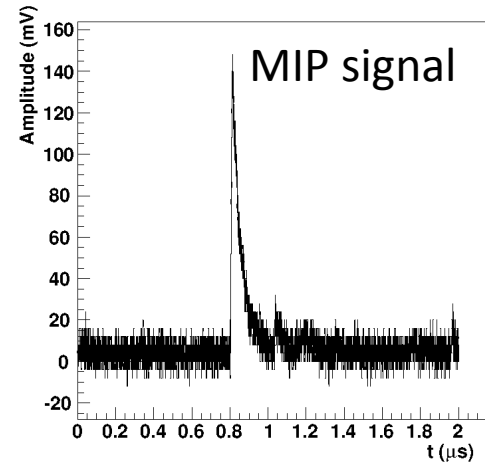
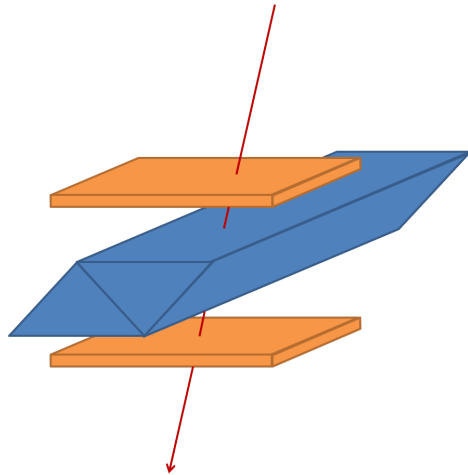


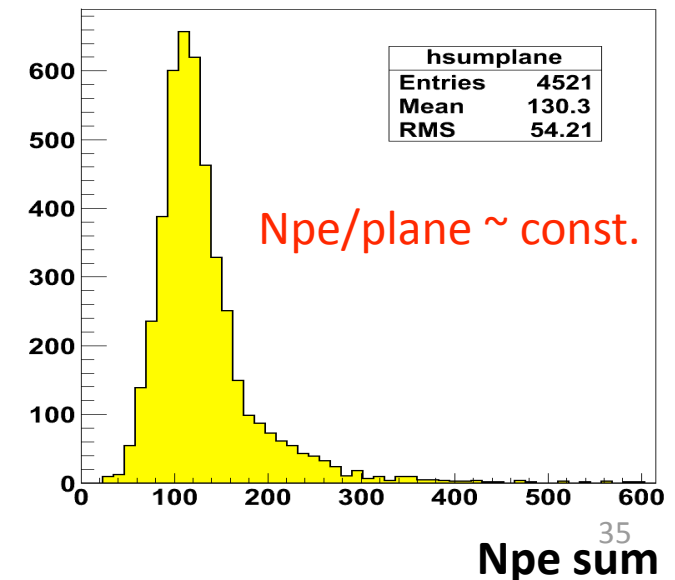
Photo-electron yield

Response to perpendicular cosmic rays with a pair of scintillators



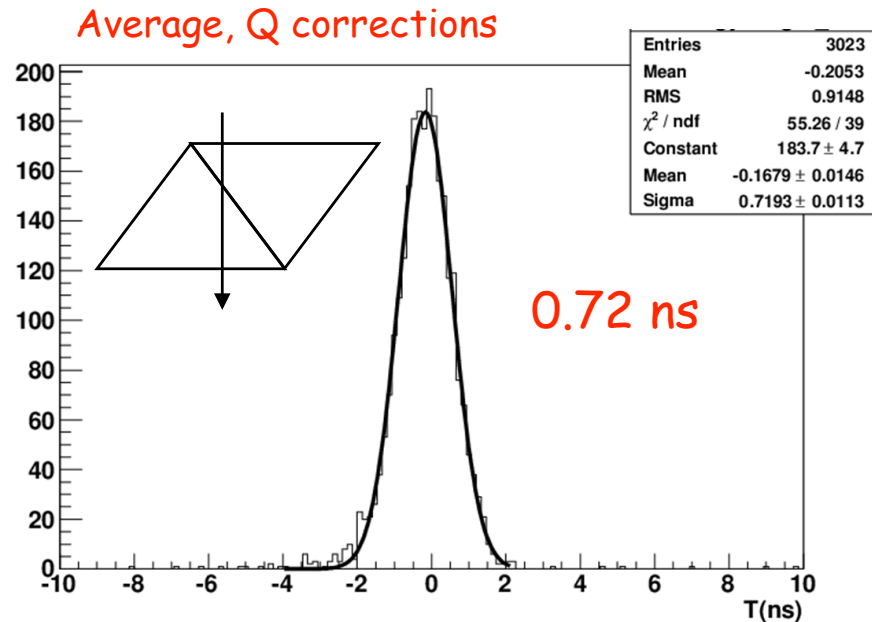
The single photoelectron charge measured using dark spectrum

- O(100) photoelectrons summing the two bars
- ~25 p.e./ MeV



Fast 20X amplification after 1.5 m coaxial cable

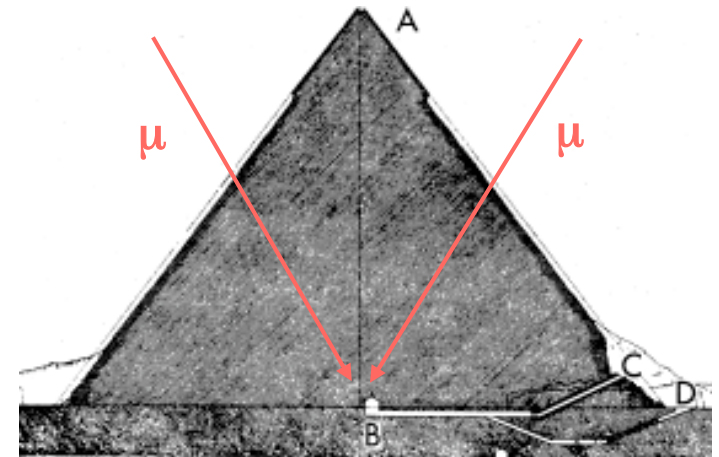
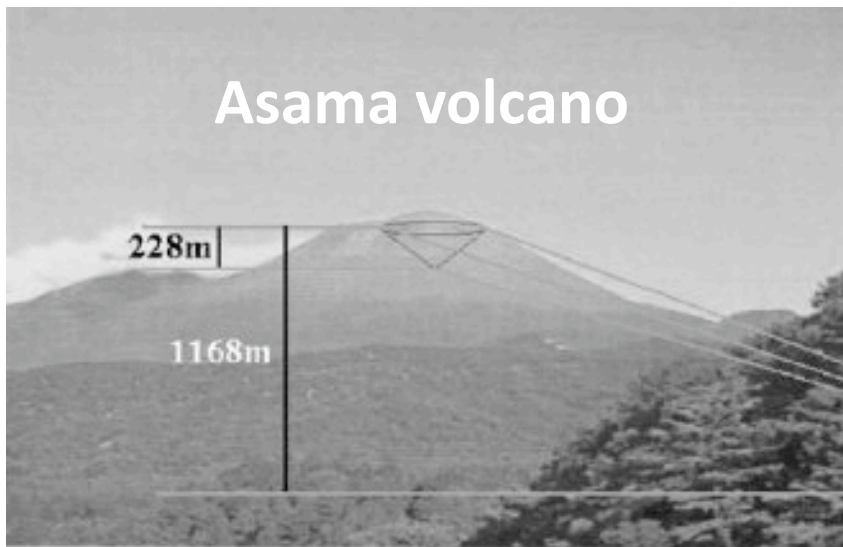
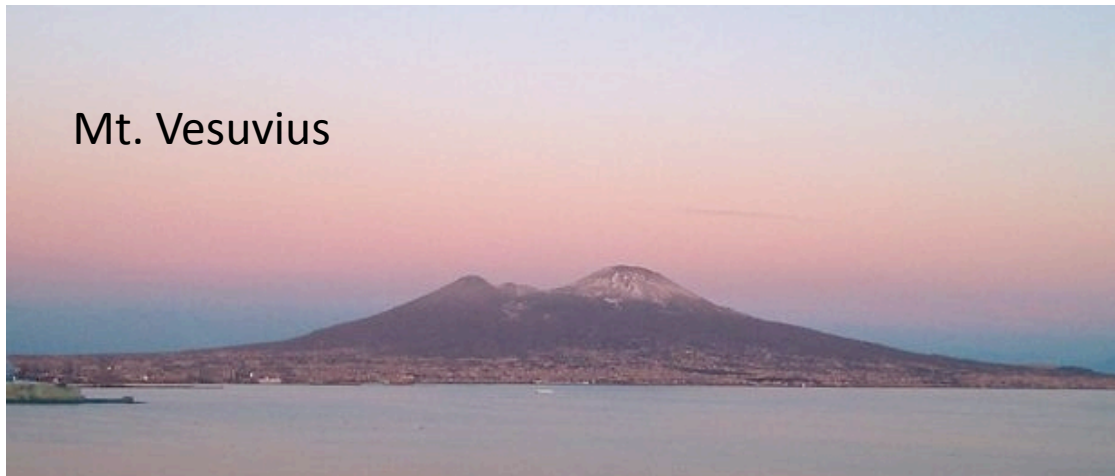
Time resolution



- After proper individual channel t_0 subtraction time of the event will be given by the first fired channel or by the average.
- Charge used for for time slewing corrections
- O(400) ps from trigger not subtracted

MU-RAY

Muon radiography with cosmic rays



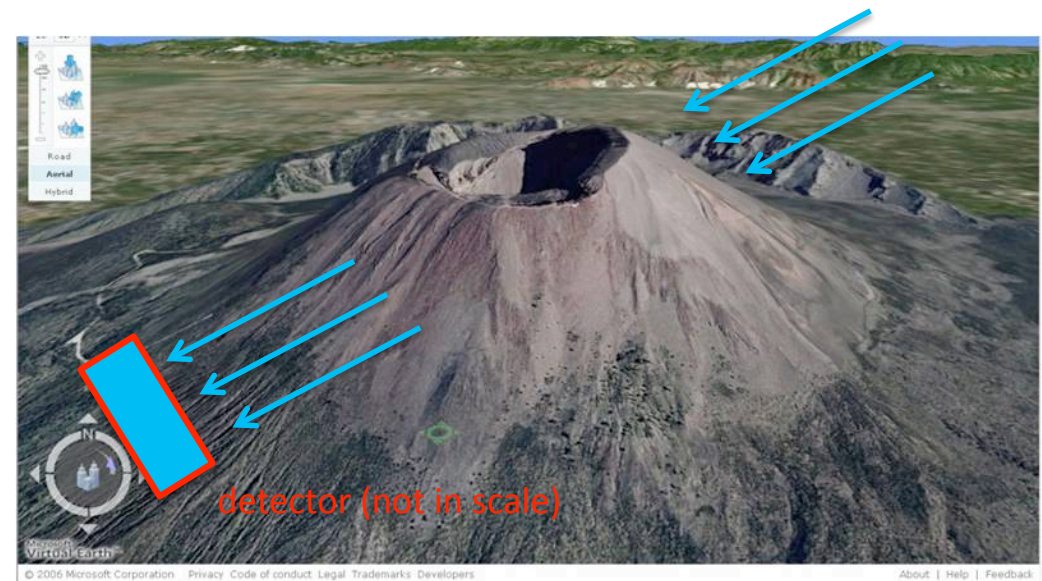
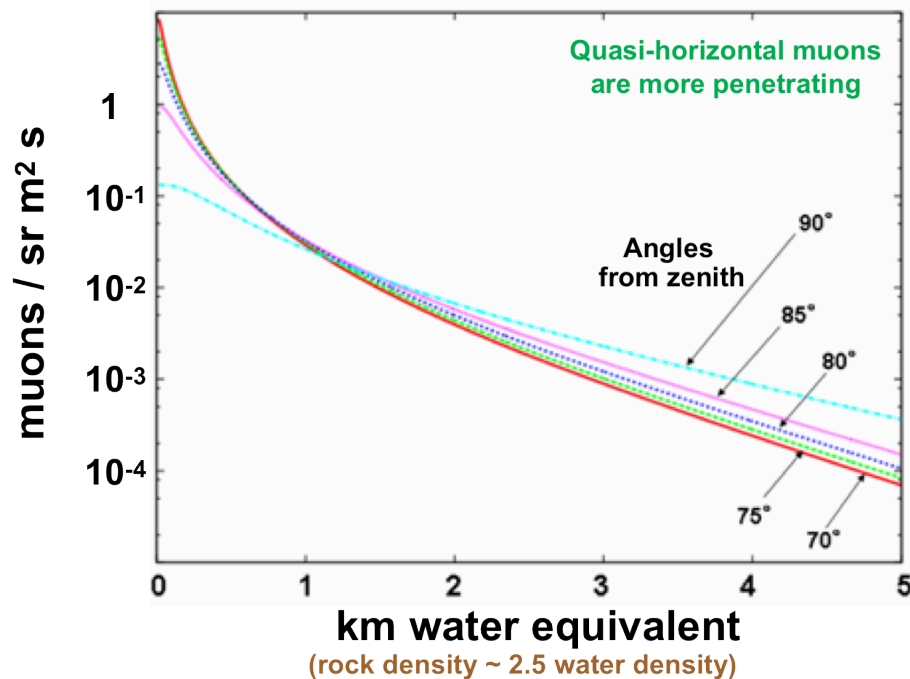
Chephren's pyramid



G. Saracino

Muon radiography principles

Cosmic muons have a deep penetration capability. Measuring the flux absorption the average density can be extracted

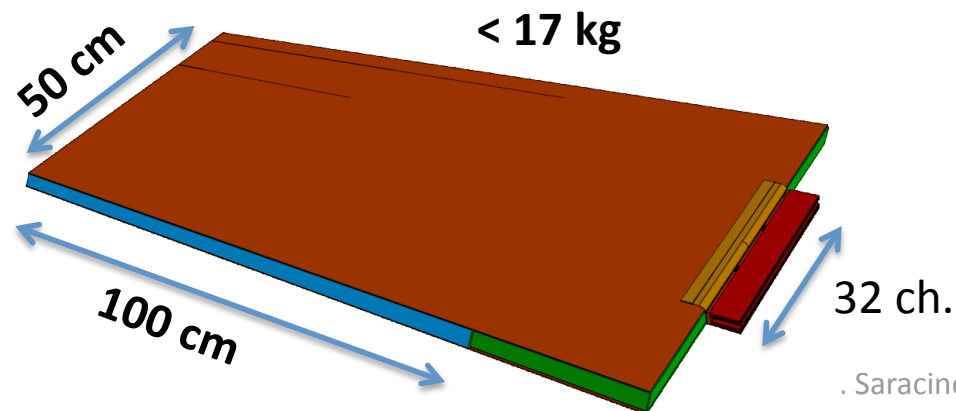


$$A_{mis}(\vartheta, \varphi) = 1 - \frac{N_{\mu}^{obs}(\vartheta, \varphi)}{N_{sky}^{obs}(\vartheta, \varphi)}$$

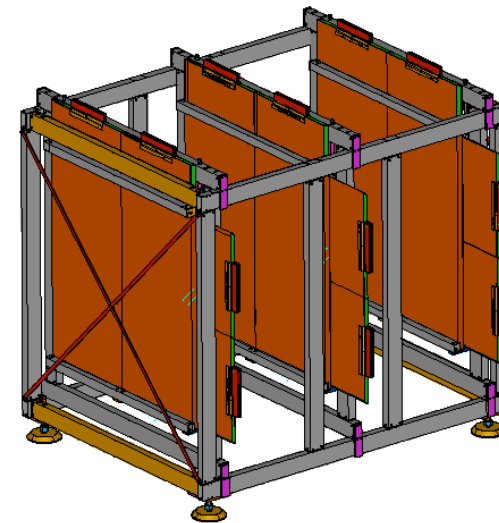
Detector design

driven by on-field requirements:
robustness, modularity and low power consumption
with particular attention to:
space and time resolutions, background rejection, large active area, low cost.

- three X-Y stations of $1 \times 1 \text{ m}^2$ sensitive area
- 12 modules easy to transport and to assembly
- Time of flight measurement
- much higher resolution than existing telescope



. Saracino

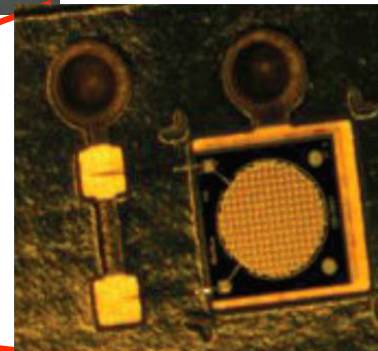
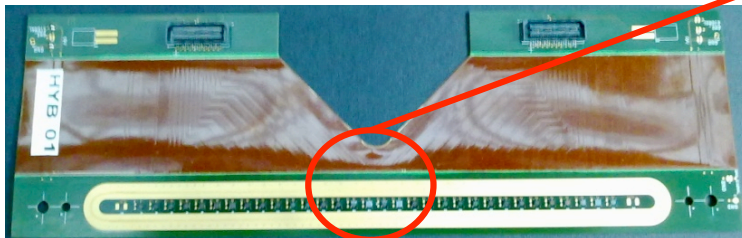
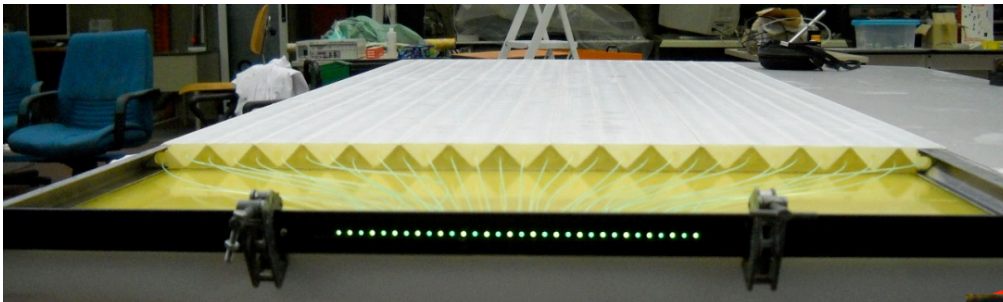


< 280 kg

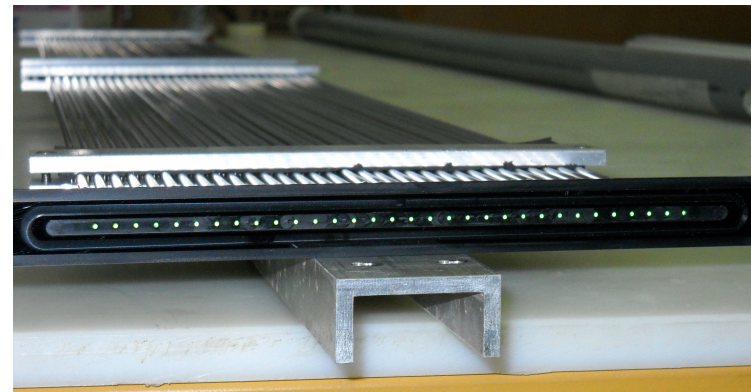
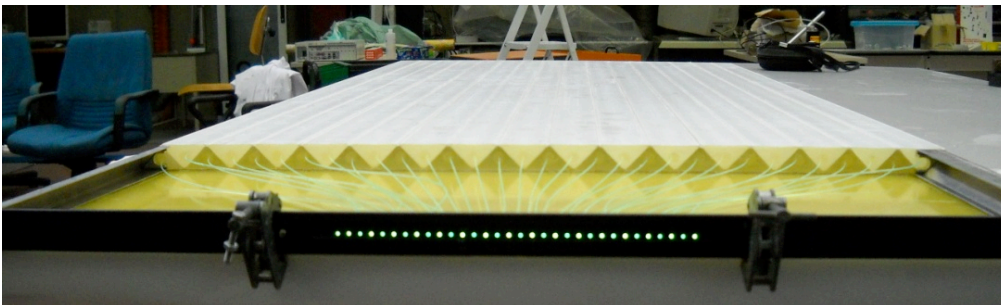
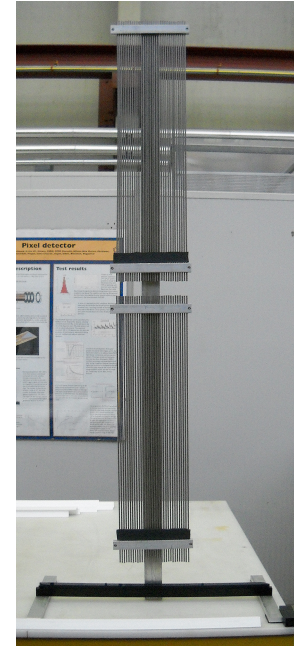
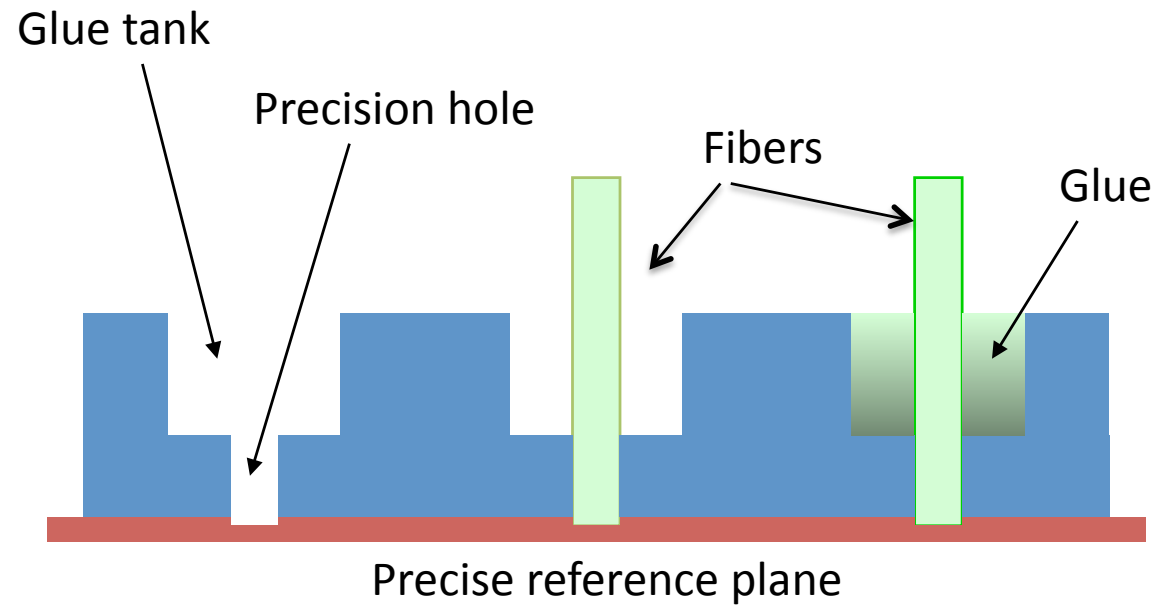
A “tabletop” experiment
all issues developed inside the
collaboration: mechanics,
electronic software etc. etc

Technological choice

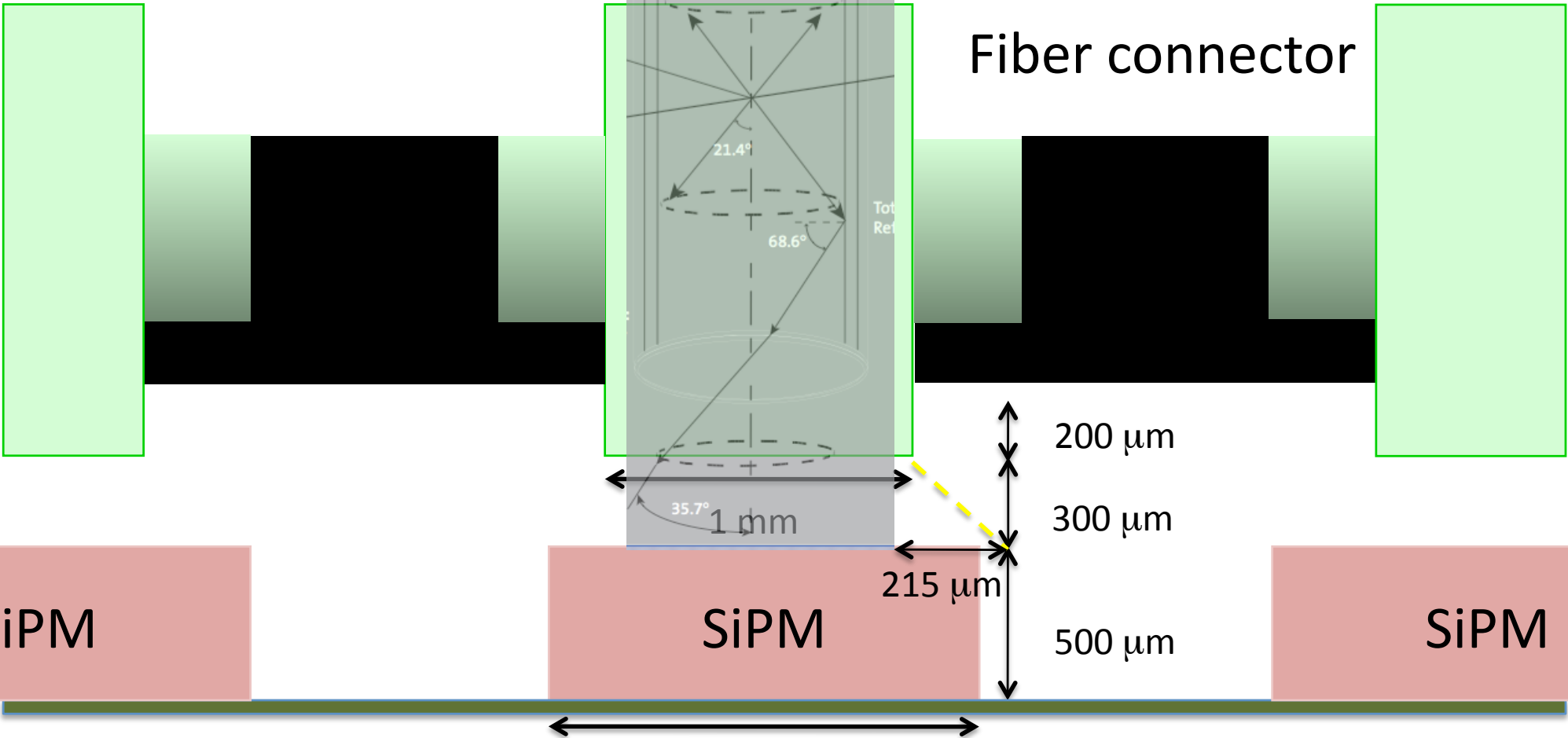
- Triangular plastic scintillator bars(D0-Minerva) : robust, fast, chip, spatial resolution.
- Fast WLS fibers photon collection
- SiPM light read-out: low power, robust , fast, chip
- One single 32-SiPMs connector to optimize cooling (power)
- SPIROC FE electronic: SiPM dedicated, low power consumption
- Dedicated low power consumption FE and DAQ electronic



Fibers connector



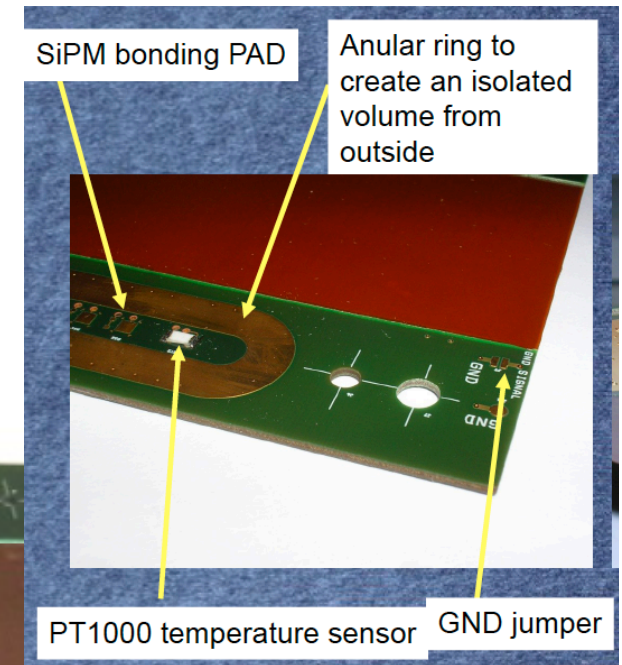
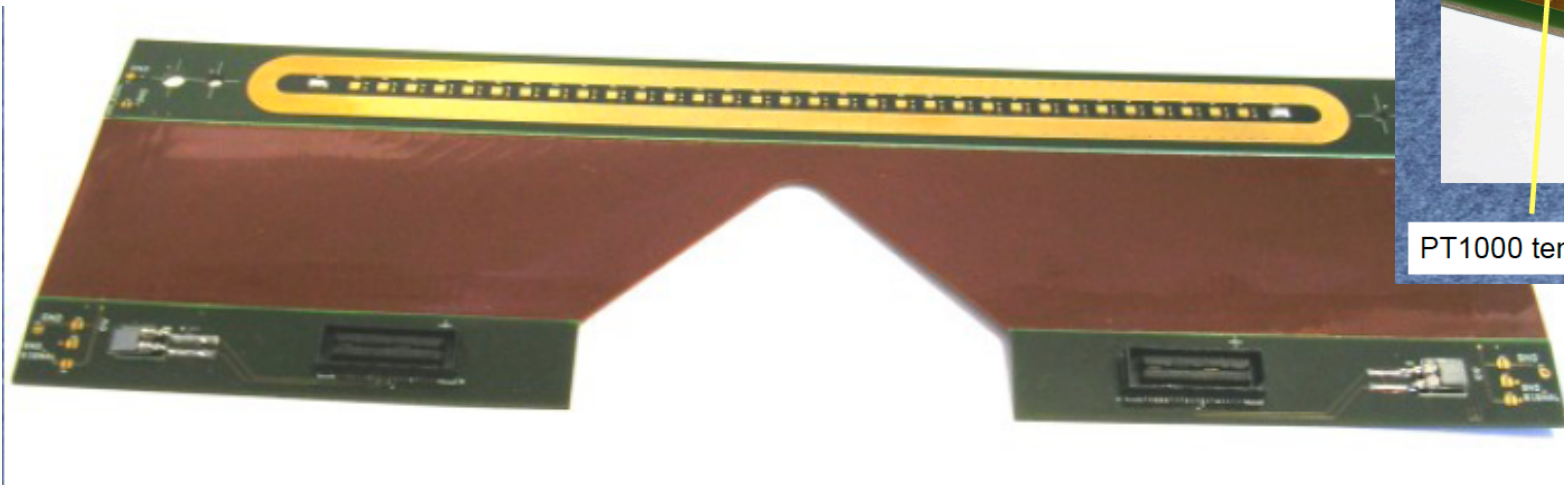
Fiber SiPM coupling



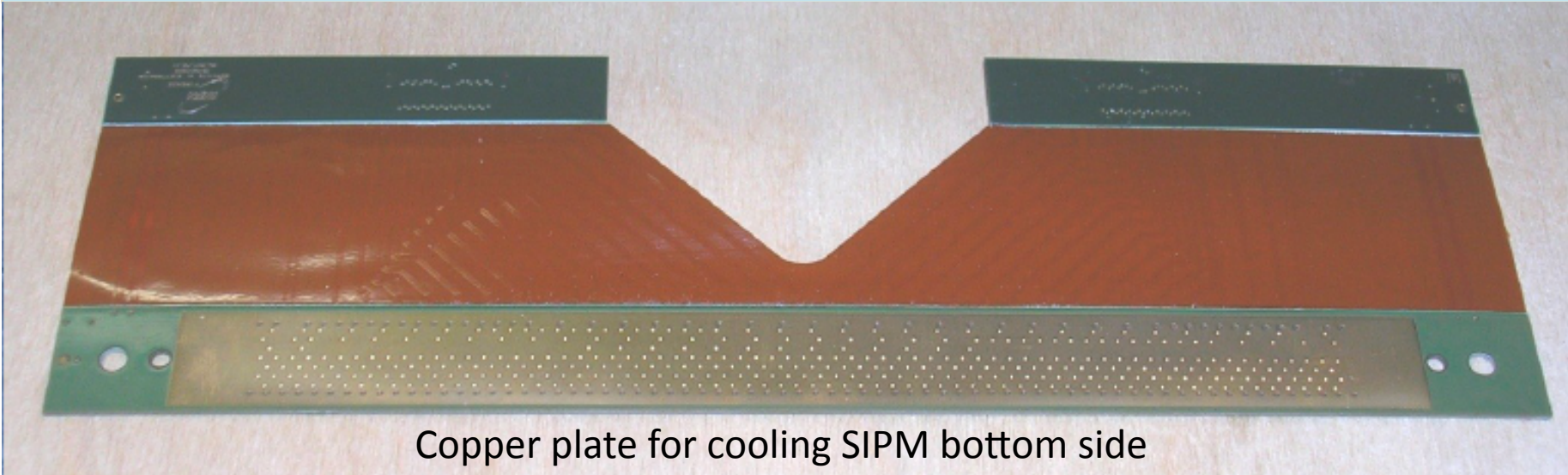
SiPM PCB

Telescope will work outdoor, SiPM temperature control is mandatory

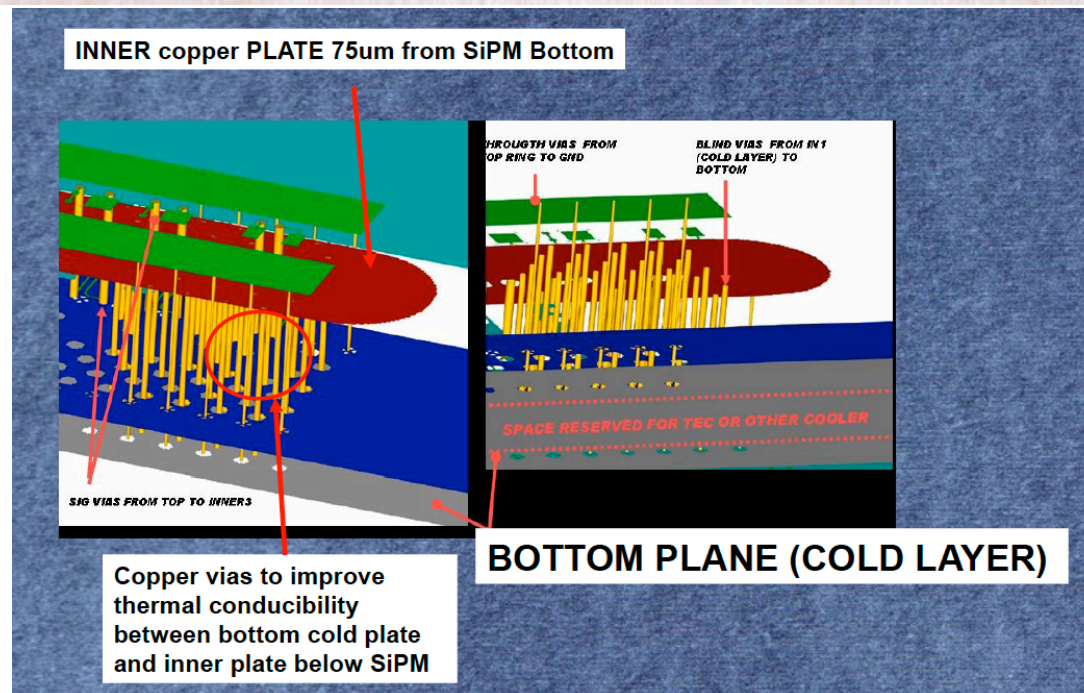
To optimize power consumption 32 die SiPM are glued on a single dedicated PCB optimized for temperature uniformity (Peltier cell)



SiPM PCB

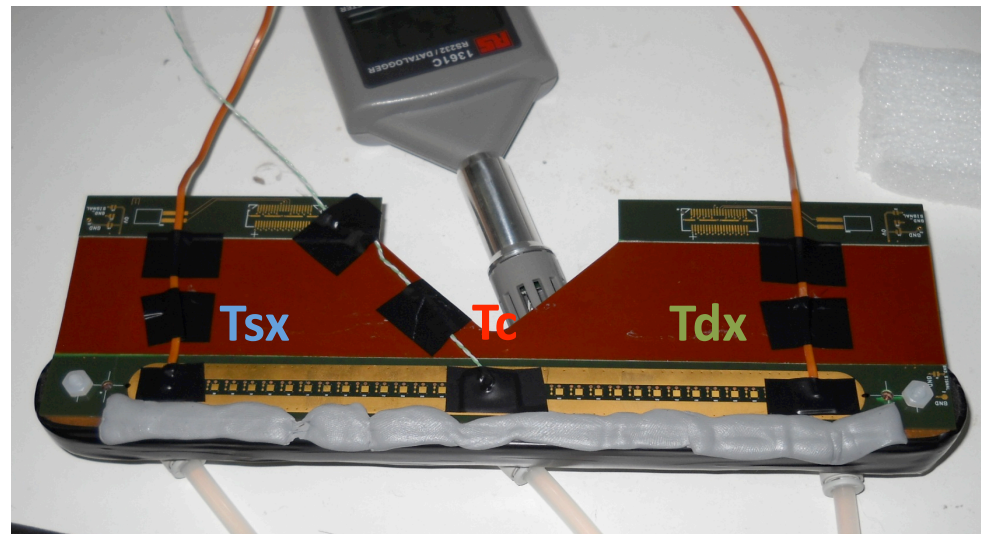
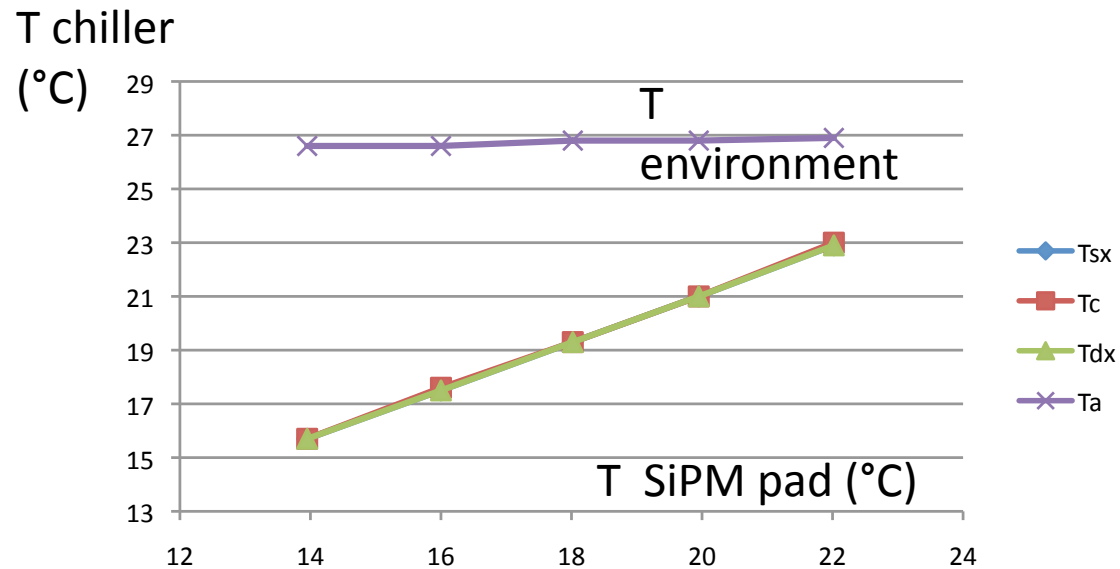


Copper plate for cooling SiPM bottom side



Hybrid temperature uniformity

Temperature differences below instrument accuracy: 0.1 °C



SiPM Temperature control (I)

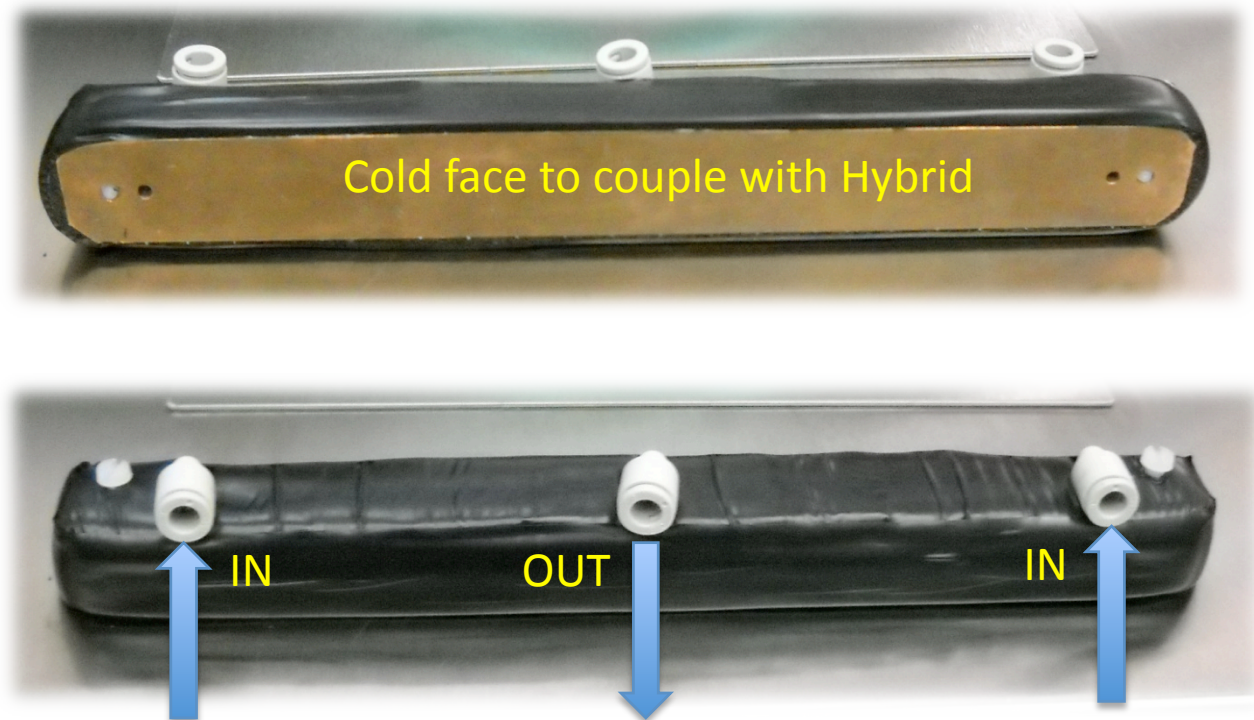
Final system: based on Peltier cell, to be optimized for power consumpt.

At the present time we developed a water chiller based system to be used when electric power is not a problem (laboratory test, Mt Vesuvius, ..)



Chiller: 0.01°C water temperature accuracy

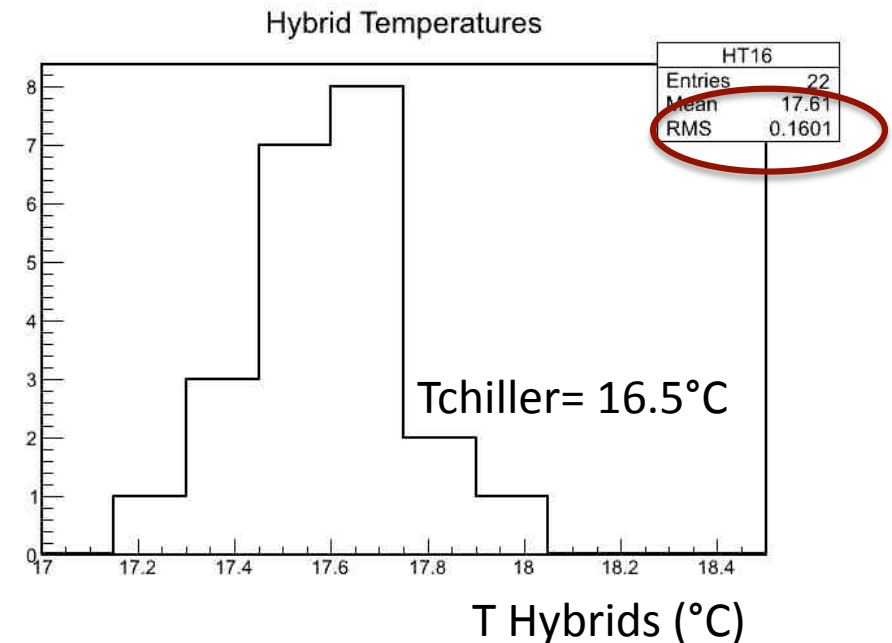
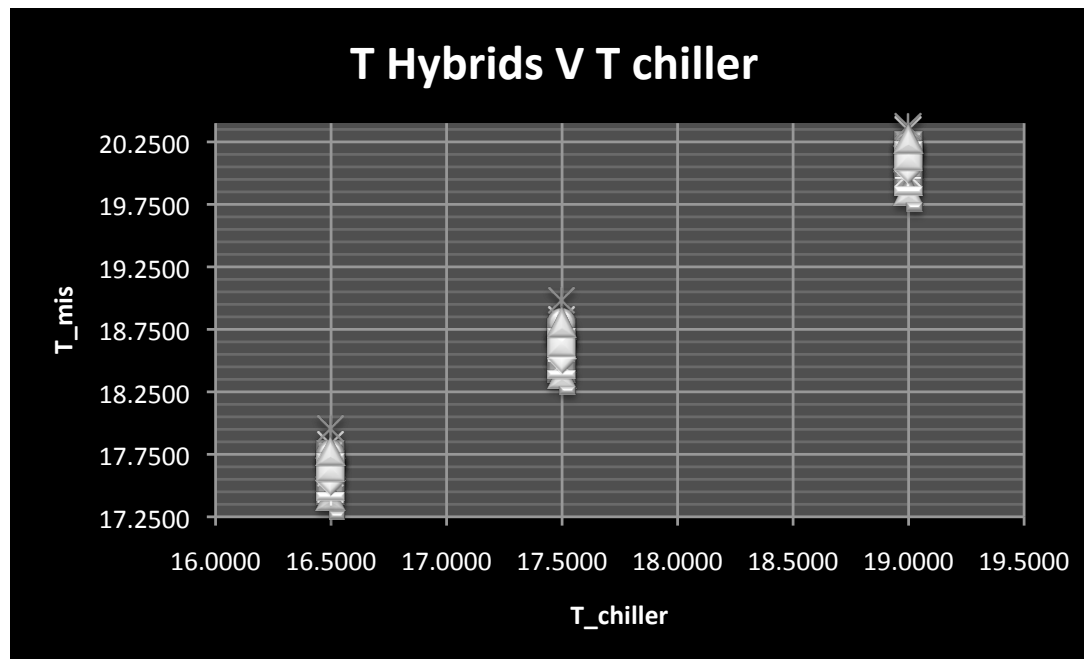
Thermal exchanger



Water inlets

SiPM Temperature control (II)

water chiller: we tested the system with all 12 hybrid mounted together

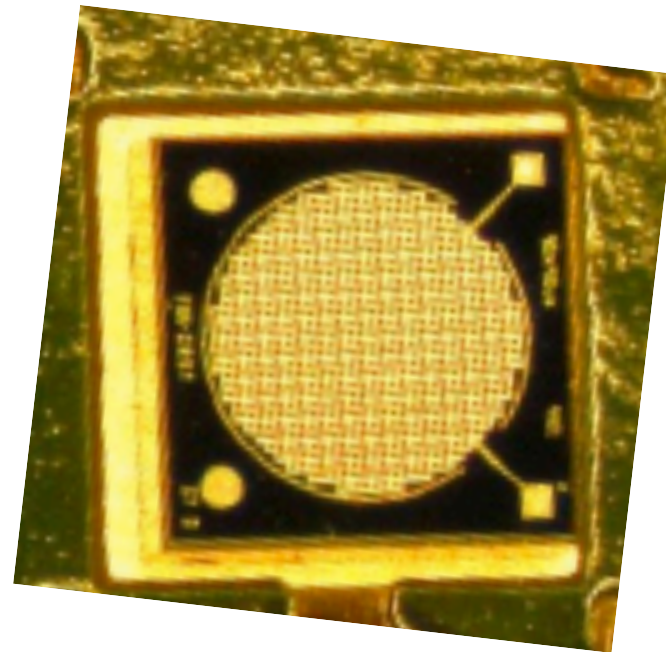
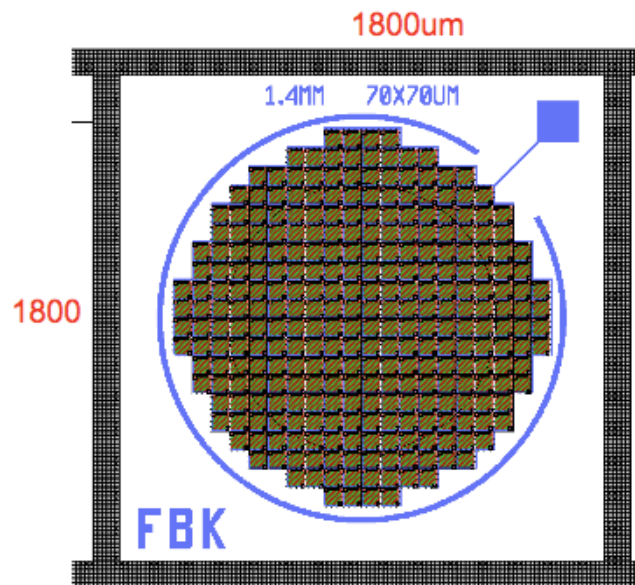


**Results are very good, Hybrid temperature RMS is 0.16 °C :
(T sensors not calibrated)**

SiPM choice

Produced by FBK-IRST in a multi-project run with MU-RAY specifics:

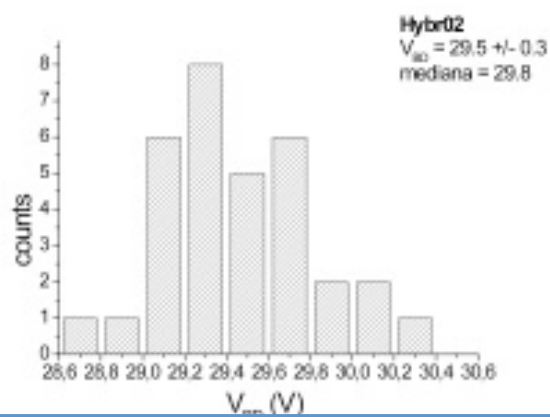
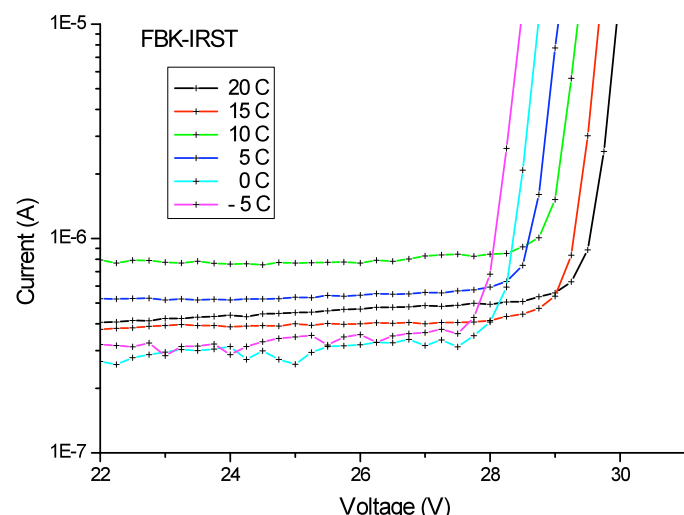
- SiPM active area: circular 1.4mm diam.
- pixel size: $70\text{ }\mu\text{m} \times 70\text{ }\mu\text{m}$ (F.F. ≈ 65)
- number of pixel: 292



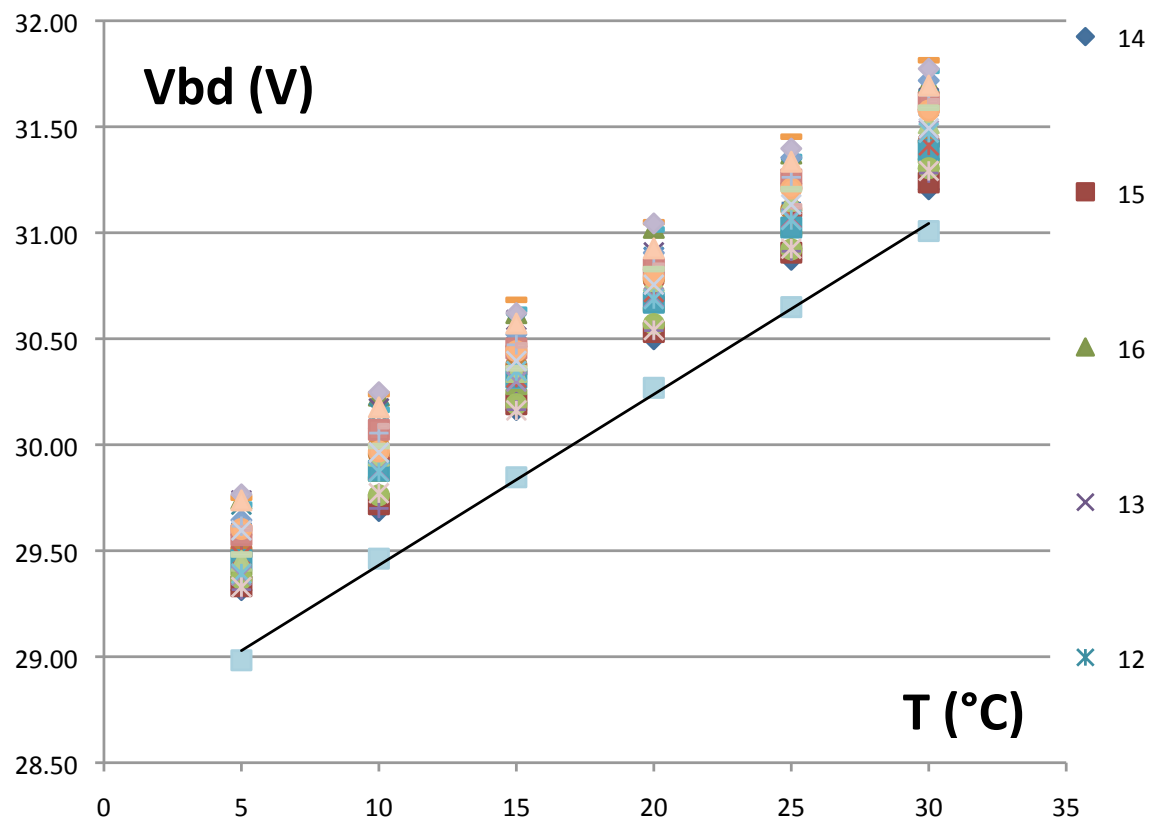
Note: when the project started (2009) few SiPM types were available on the market. Hamamatsu doesn't provide die chips and array were just at the beginning.

I-V reverse bias: $V_{bd}(T)$

A linear trend has been measured in the temperature range $+5 \div +30$ °C



The slope is similar for all the SiPM: ≈ 80 mV/°C

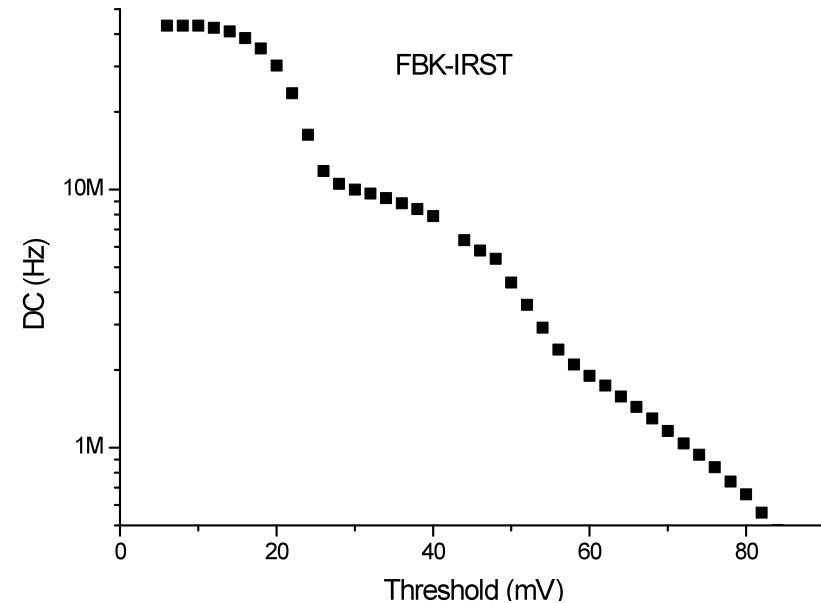
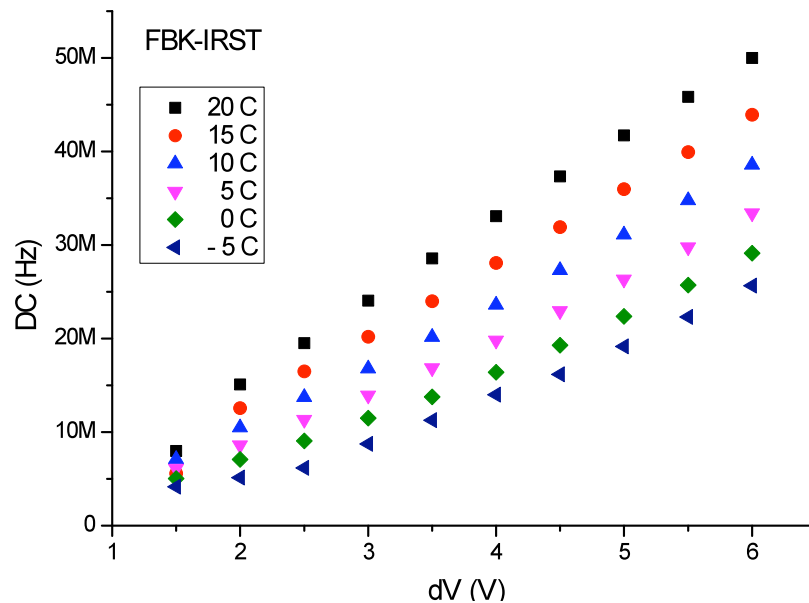


SiPM can work at different, constant, temperatures to optimize cooling power consumption

Dark Counts

Dark rates up to 40 MHz !!

DC at 20 C DV =5,5 V



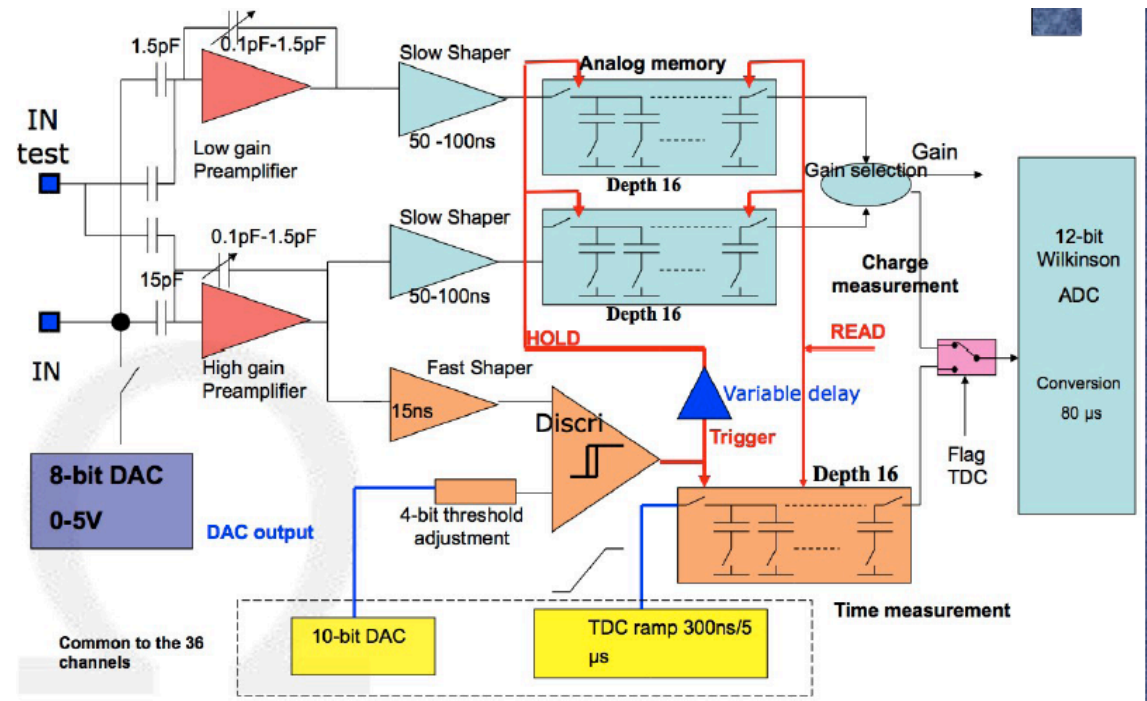
O. Starodubtsev RD11

F.E.E.: SPIROC ASIC

(SiPM Integrated Read Out Chip): Dedicated very front-end electronics for an ILC prototype hadronic calorimeter with SiPM readout (CALICE). Designed by OMEGA-LAL group of Orsay

Main features:

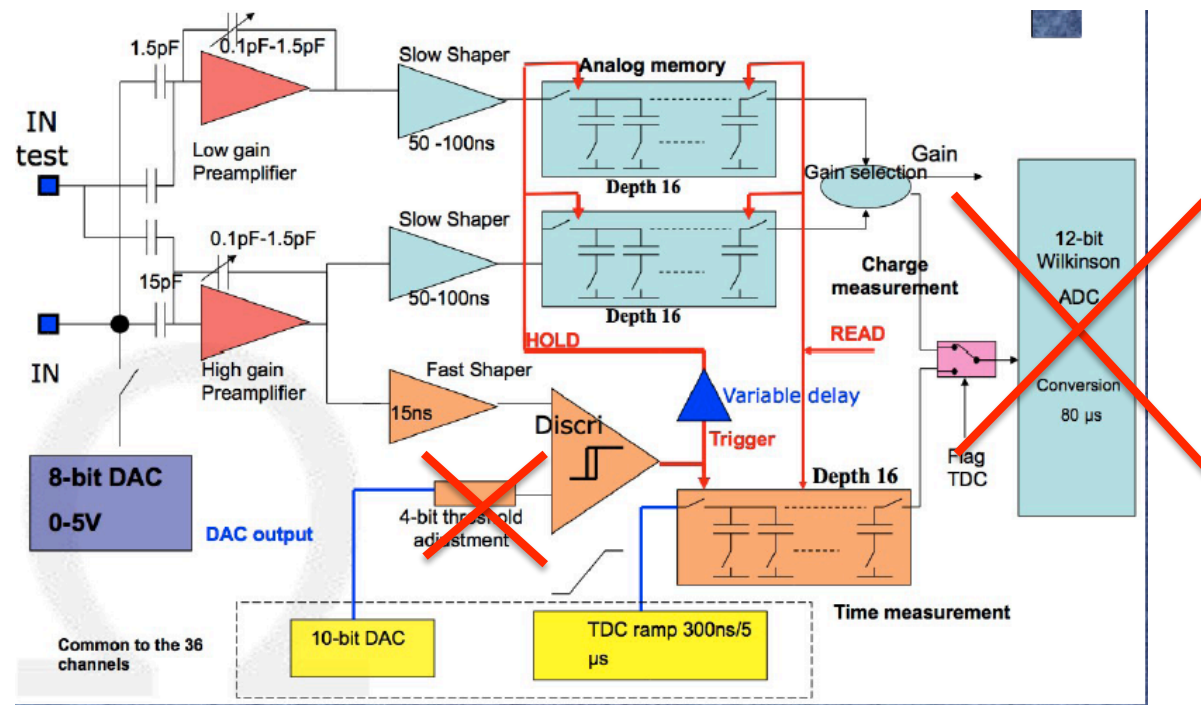
- 36 channels
- Individual fine bias voltage (0-5 V)
- FAST OR 36 available as digital output
- Energy measurements: 2 gains/12 bit internal ADC 1p.e. \rightarrow 2000 p.e. range pe/noise = 12
- internal TDC 100 ps resolution
- low power cons.: 25 μ W/ch in idle mode
- TDC auto trigger available



MURAY F.E.E.

The MURAY telescope must work in self-trigger mode

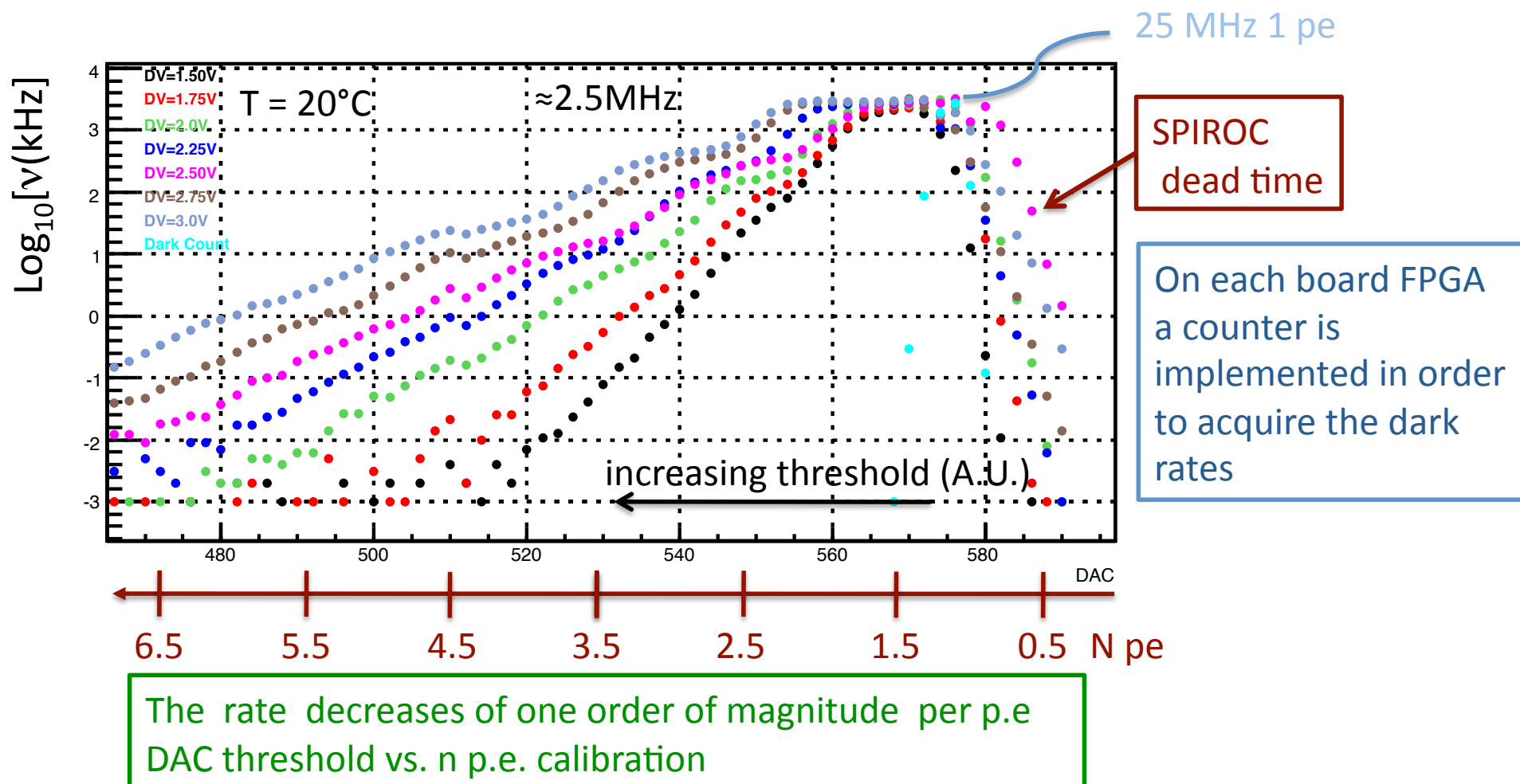
In 2009 the first production of SPIROC was available, some features were not working



In particular time and charge measurement have to be implemented in the board

S curve

Discriminator thresholds vs. dark rates calibration



Telescope structure

Distance among planes can be changed.
The whole structure can be easily rotated for free-sky calibration



Telescope commissioning

The telescope has been mounted in the laboratory, working with vertical muons



Conclusions

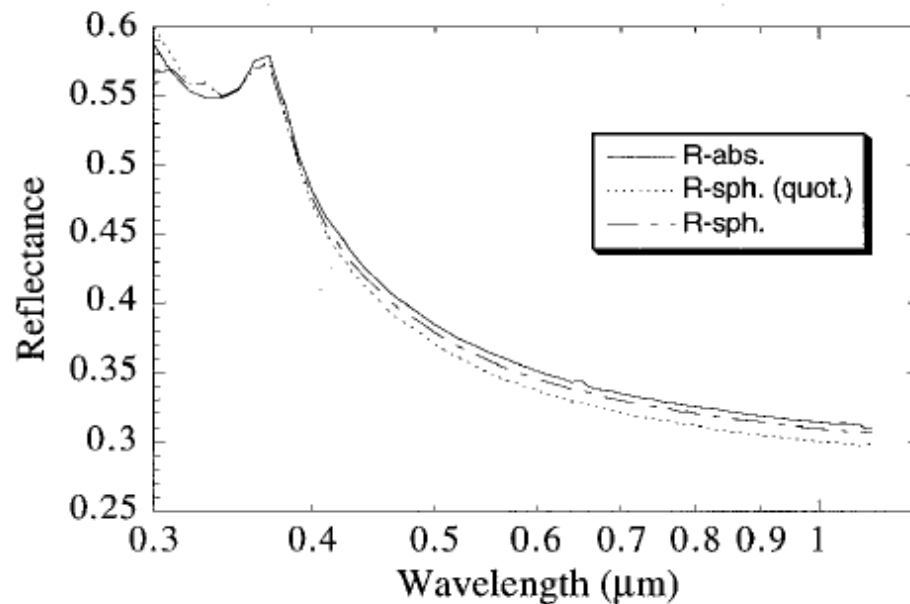
- SiPM started to be used in more and more applications, in HEP and not only
- The number of producers is increased greatly in the last years as the number of SiPM models available on the market
- SiPM are still a novel technology: many improvements expected in the next years

SPARES

Photons reflection, conversion and absorption in Si

Photons impinging on a silicon sensor can undergo one of the following processes:

- Surface reflectivity losses
- Absorption losses in the top protection layer
- Absorption losses in the cell separations (for SiPM)
- Conversion inside the top high conductive layer p^{++} layer with rapid recombination (UV light)
- Conversion in the depleted p-n junction (with e/h triggering eventually an avalanche in SiPM)
- Conversion in the un-depleted n-layer (IR light)
- No absorption at all (long WL IR light)



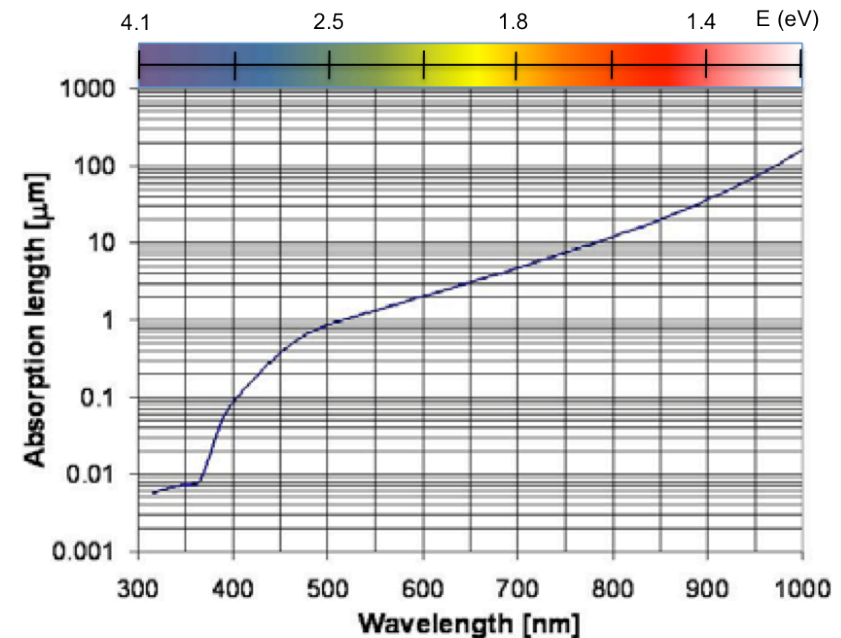
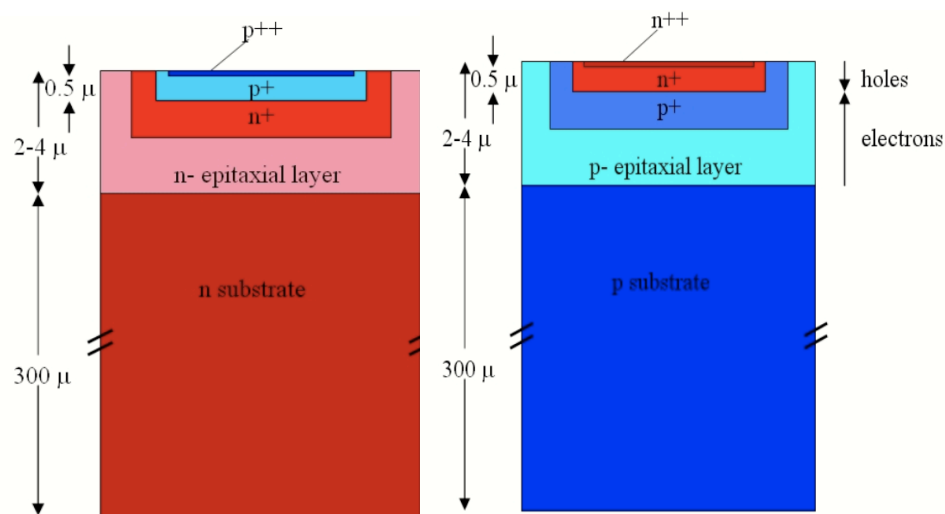
For Si $n = 3.5$: a large fraction of photons is reflected
A thin SiO₂ can cover the diode ($n = 1.46$):
Special antireflective coatings can reduce below 10% the reflection losses
Passivation layers have very high optical quality, except in the UV region below 300 nm

Quantum efficiency

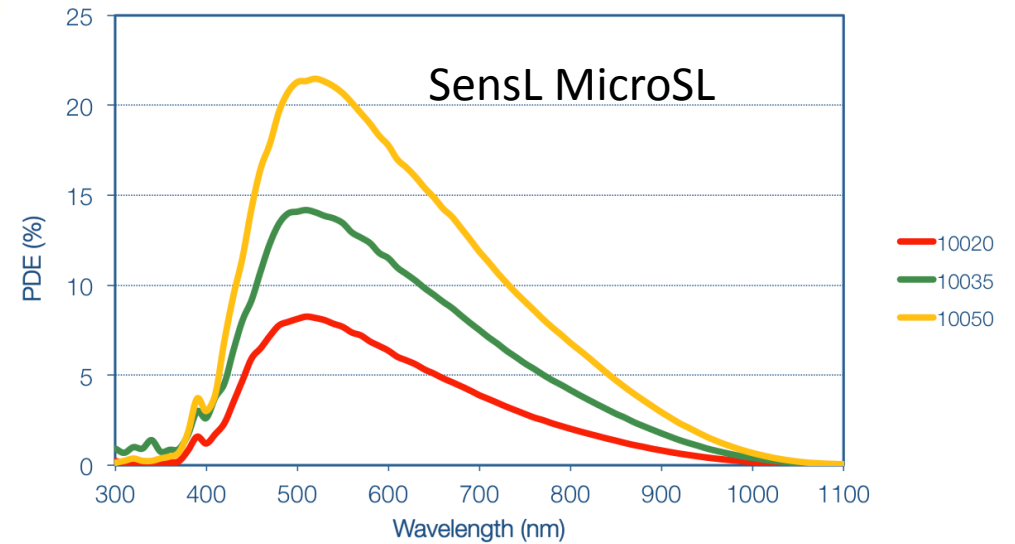
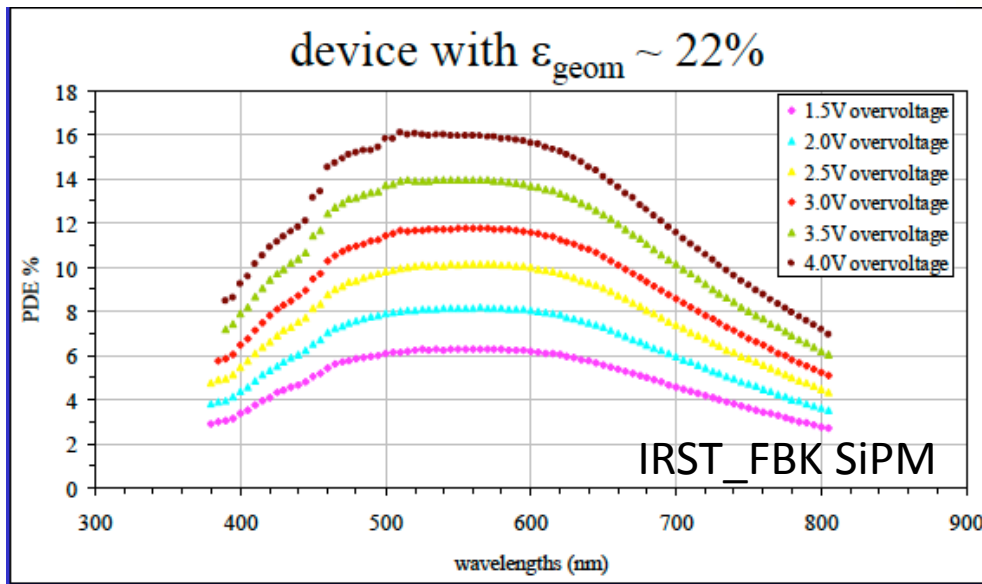
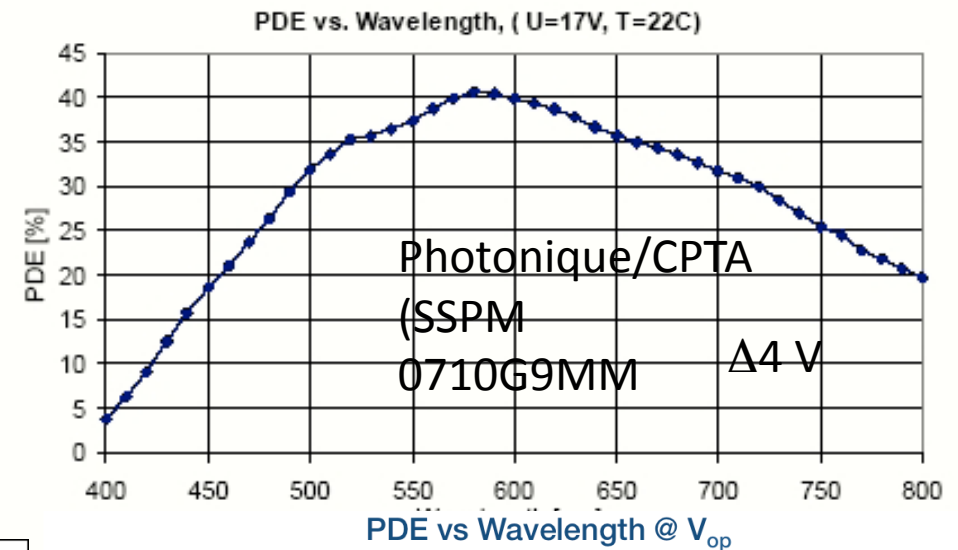
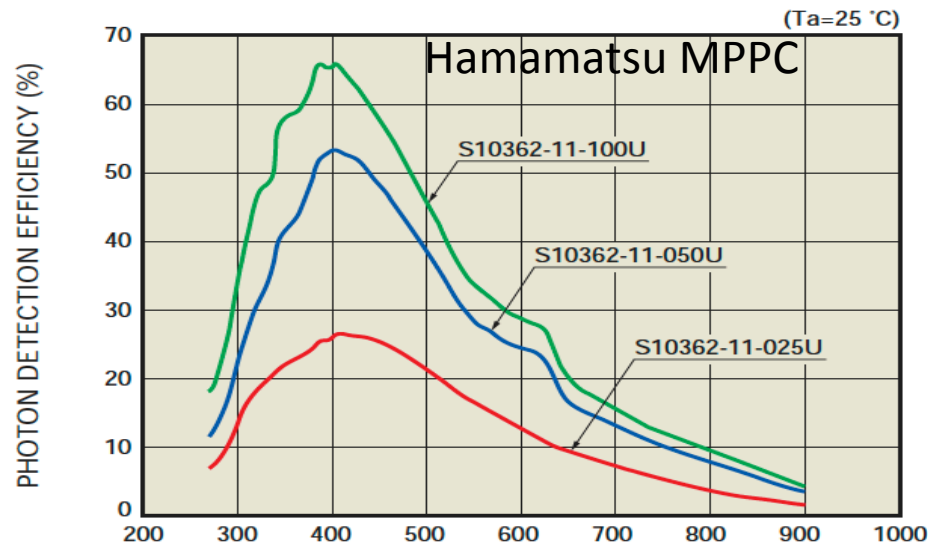
QE is related to absorption length

SiPM sensitive layer is very thin (few microns), and the junction side facing to the surface is few tenths of micron.

Depending on the kind of technology p-on-n or n-on-p the QE efficiency is peaked at different wave-length: blue for p-on-n, green for n-on-p

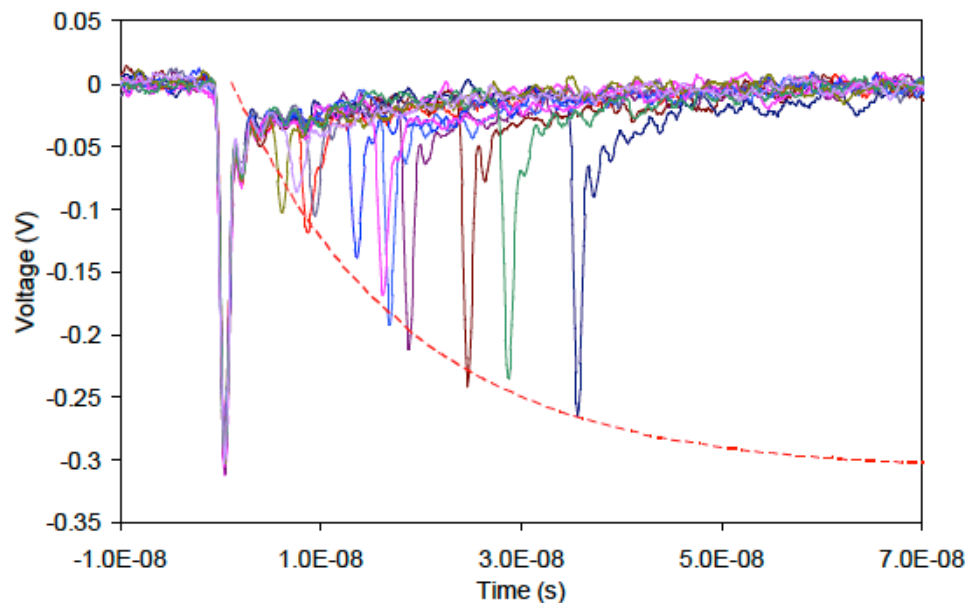


PDE curves



After-pulsing

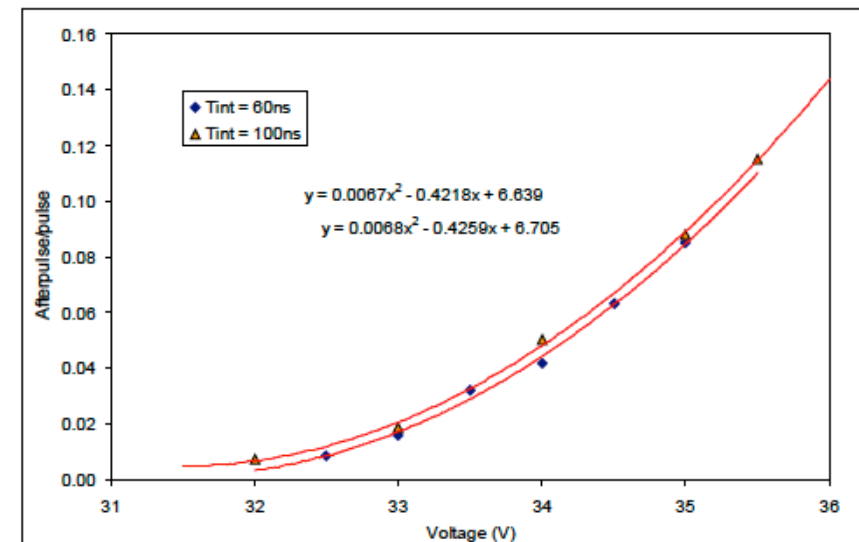
Once a cell has fired there is a probability that it fires again, due to the trapping of carriers that can be released with a characteristic time $\tau \approx 100$ ns
Since the cell requires some time to recharge after breakdown, after-pulse amplitude depends on the time



If integration time is comparable to τ
charge is systematically overestimated

(C. Piemonte: June 13th, 2007, Perugia)

7/3/12



Trigger probability is a quadratic function of the overvoltage: $P = P_C \times P_t$

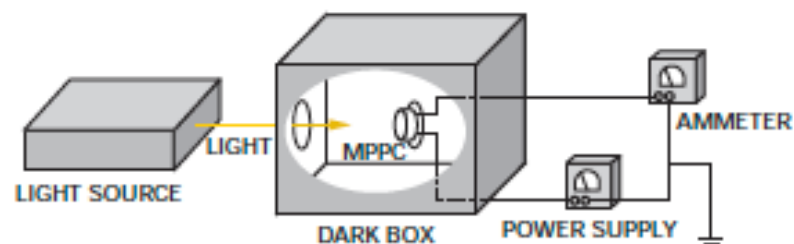
P_C = trap capture probability: depends by the number of carriers, i.e. by gain linear

P_t : trigger probability linear in V_{bias} (before saturation)

About PDE measurements (I)

From Hamamatsu datasheet

[Figure 14] Measurement setup for MPPC photon detection efficiency (using monochromator)



$$\text{PDE} = \frac{\text{Number of photons detected by MPPC}}{\text{Number of photons incident on photodiode}} \times \frac{\text{Photodiode active area}}{\text{MPPC active area}} \dots (5)$$

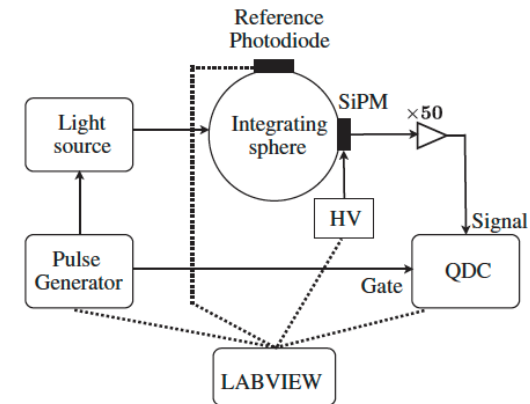
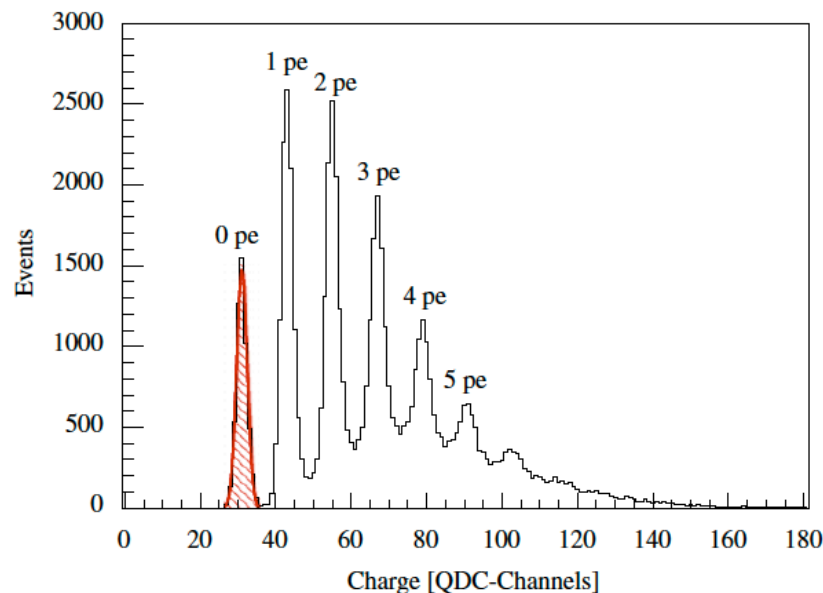
Note: Since the number of photons detected by the MPPC is calculated from the photocurrent, the photon detection efficiency obtained by the above equation also takes into account the effects from crosstalk and after-pulses.

The integrated charge is measured, which overestimates the number of cells fired by photons, containing contribution from X-talk and after-pulsing (see later....)

About PDE measurements (II)

Using a low emission pulsed light source the real number of pe can be measured for some WL

$$P(0, n_{pe}) = e^{-n_{pe}} \rightarrow n_{pe} = -\ln(P(0, n_{pe})) = -\ln\left(\frac{N_{ped}}{N_{tot}}\right) + \ln\left(\frac{N_{ped}^{dark}}{N_{tot}^{dark}}\right)$$



4 absolute PDE measured to
normalize the curve
465, 633, 775 ND 870 NM

P. Eckert et al. / Nuclear Instruments and Methods in Physics Research A 620 (2010) 217–226

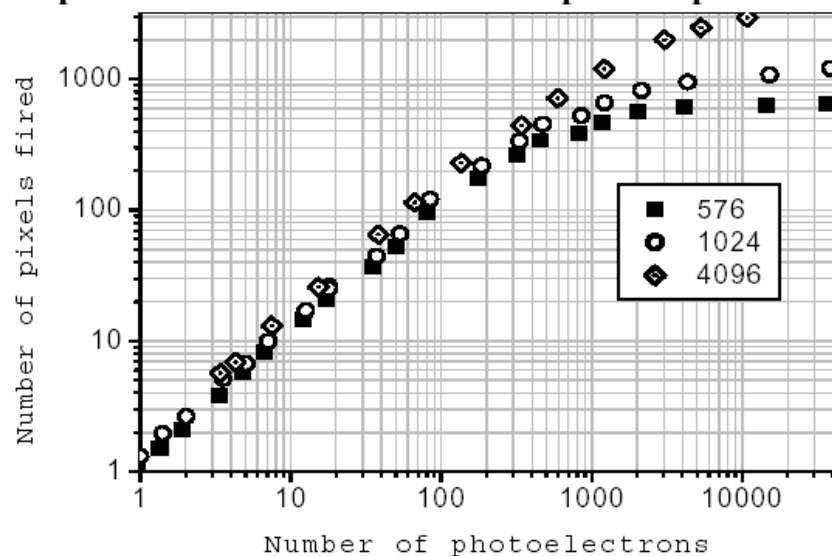
SiPM linearity

The single cell is a “digital” device, the amplitude of the signal A is independent on the number of photons impacting on it.

Since the cells are connected in parallel, the linearity is obtained by summing signal from different cells, once the number of firing cells is smaller than the number of cells

$$A = \sum A_i \approx N_{\text{cell}} (1 - \exp^{-(N_\gamma \cdot \text{PDE}) / N_{\text{cell}}}) \approx N_\gamma \cdot \text{PDE} \quad N_\gamma \cdot \text{PDE} \ll N_{\text{cell}}$$

Response functions for the SiPMs with different total pixel numbers measured for 40 ps laser pulses

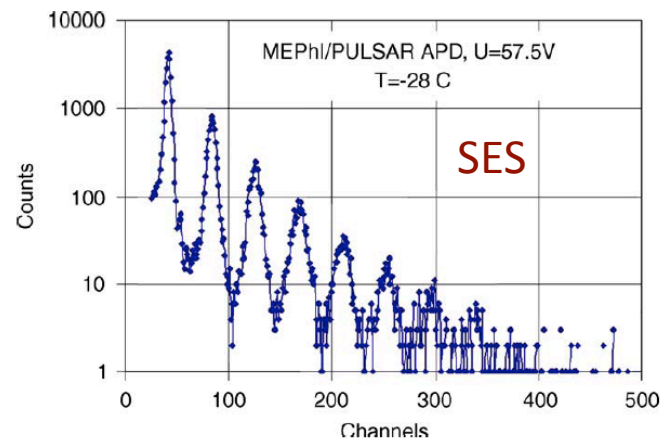
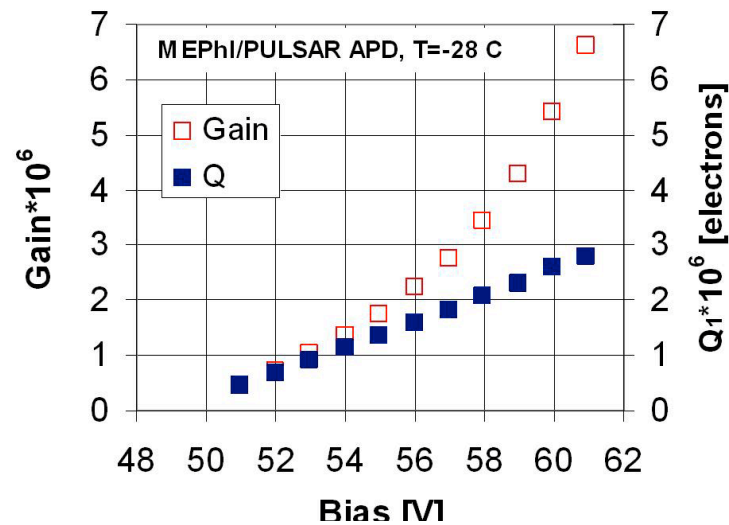


This formula doesn't take in account X-talk and after pulsing they introduce an Excess Noise Factor with respect to the ideal SiPM

V. Andreev et. al., Nucl. Instrum. Meth. A 540 (2005) 368.

Excess Noise Factor

The effect of cross-talk and after-pulsing introduce an excess noise factor.



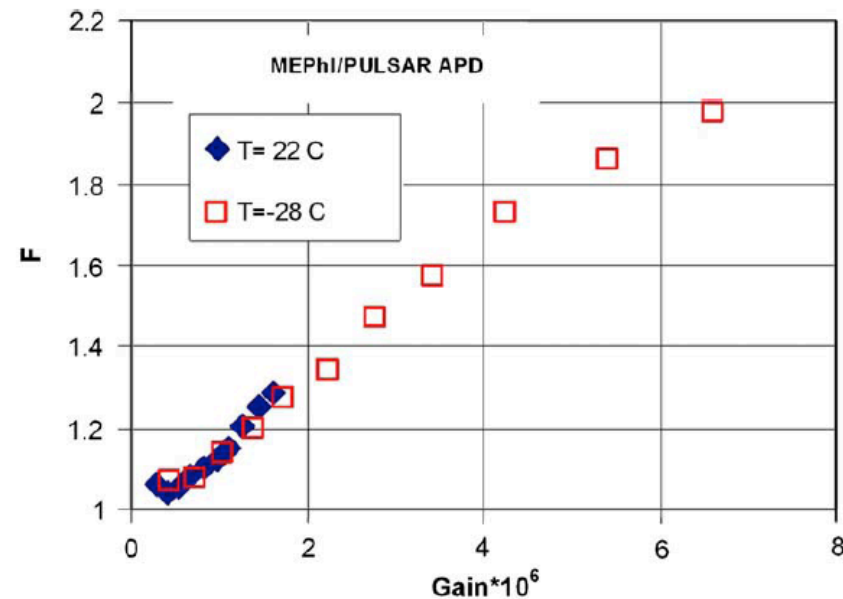
Musienko et al.: NIMA 567 (2006) 57–61

The SiPM gain can be now defined as:

$$M = \langle N_{\text{pix}} \rangle \times Q_1$$

ENF F is defined as $F = 1 + V(M)/M^2$

where mean and variance are evaluated from SES



Dark counts (I)

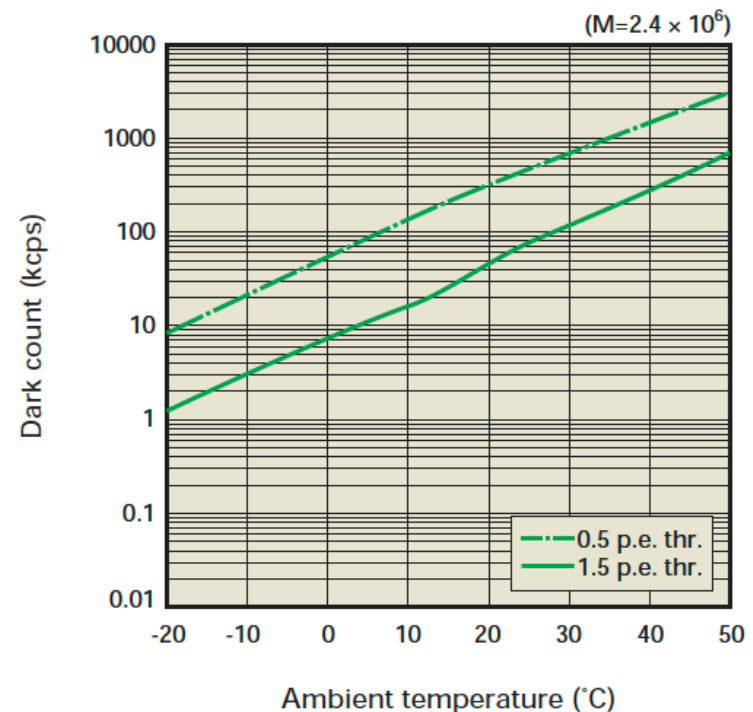
Still in absence of light we can observe signals called dark current or dark counts.

Free carriers can be produce mainly in two way

- thermally: they can be reduced by cooling (factor ≈ 2 reduction every 8 °C drop)
- field assisted generation: lower than therm. but can be reduced only by reducing the E field

Dark counts strongly depend by the SiPM production process, due to the impurities and crystal defects, and in general to the number of generation-recombination center
typical ranges are 100 kHz to several MHz per mm² at 25°C

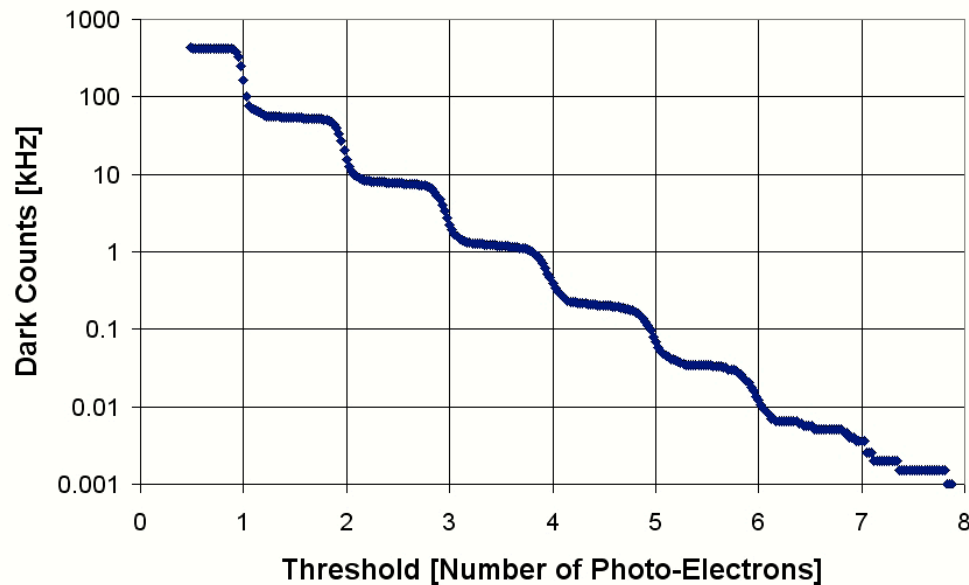
(c) S10362-11-100U/C



Dark counts (II)

As mentioned the dark spectrum shows a relevant presence of amplitudes higher than 1 cell, as expected for purely thermal generation. This is due to the optical cross-talk.

The empirical law is that this rates can be reduced of one order of magnitude increasing thresholds of one photoelectron equivalent

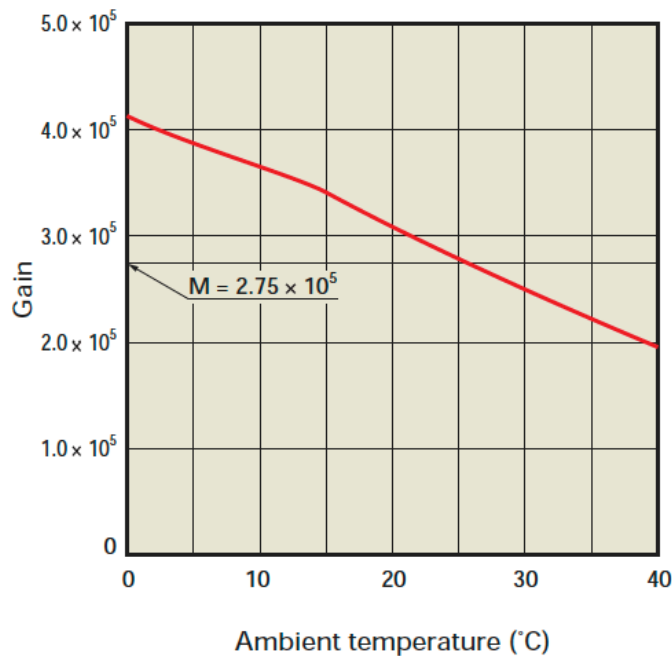


Temperature dependences (I)

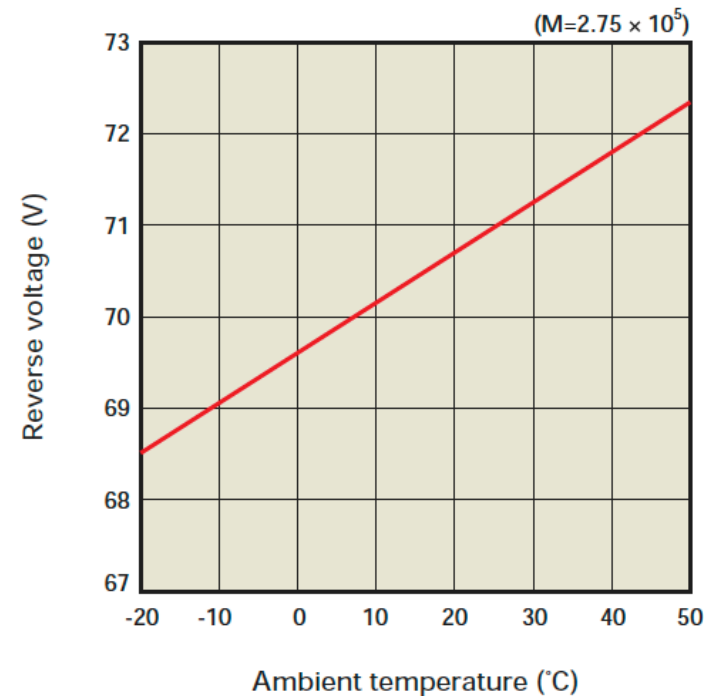
SiPM can work fine at room temperature, if dark counts are not a problem.
But they are sensitive to temperature changes! The main issue is the change of V_{bd} .
If V_{bias} is not changed, the change in temperature leads to change in gain and PDE

$$kT = dA/dT * 1/A \approx 0.3\%/^{\circ}\text{C}$$

Hamamatsu S10362-11-025U/C



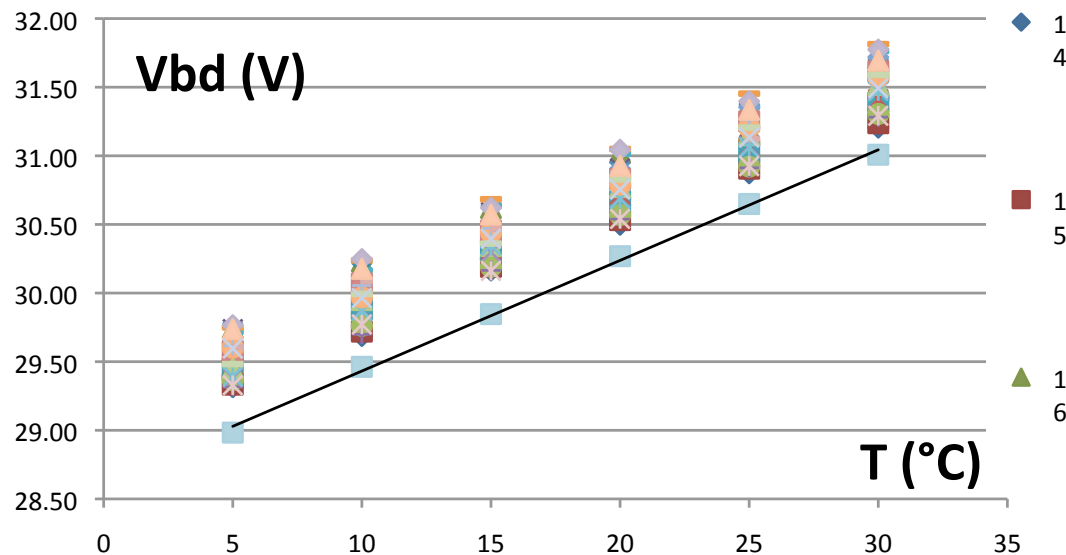
Gain change at fixed V_{bias}



V_{Bias} change at fixed gain

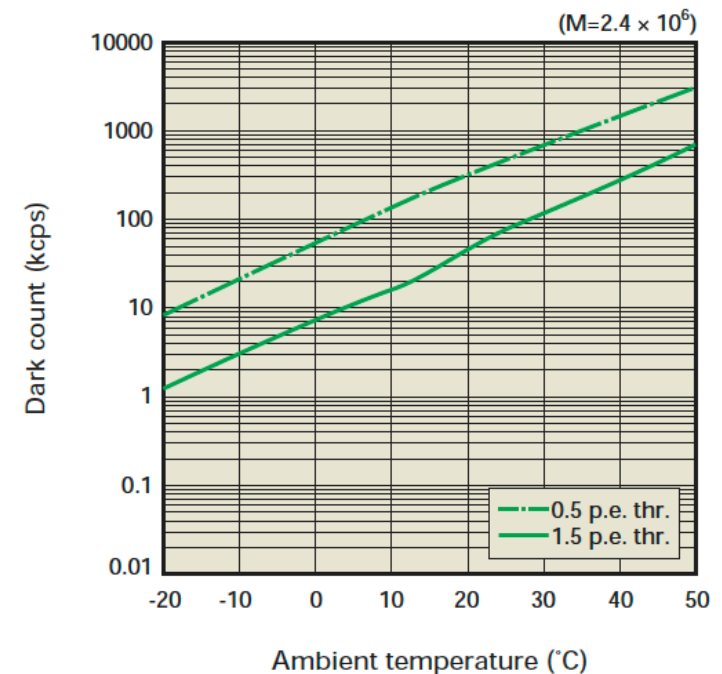
Temperature dependences (II)

Change in temperatures can be compensated by a Vbias change in order to leave VBias-Vbd constant. All relevant parameters (G,PDE) remain constant but the dark rate.



$$\text{IRST } dV_{BD}/dT = 70 \text{ MV}/^{\circ}\text{C} = 0.23 \text{ } \%/^{\circ}\text{C}$$

(c) S10362-11-100U/C



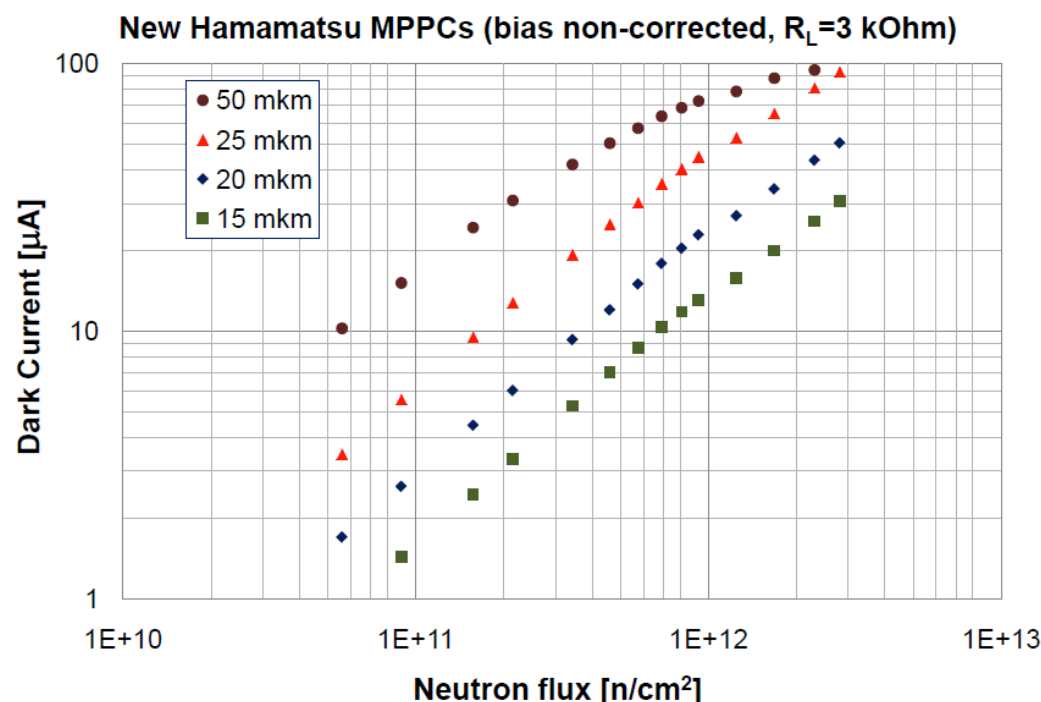
$$dV_{bd}/dT = 50 \text{ mV}/^{\circ}\text{C}$$

Radiation hardness (I)

Major concern for harsh radiation environments, typical of some HEP experiment (LHC, ILC, SuperB)

Is well known that radiation can produce defects in Si bulk or at the Si/SiO₂ interface changing the doping concentration and causing charge-trapping effects.

Possible effects on the SiPM are change of dark and leakage currents, V_{bd}, PDE.



The damage is proportional to the effective volume: $V = S \times FF \times d$

S= surface area

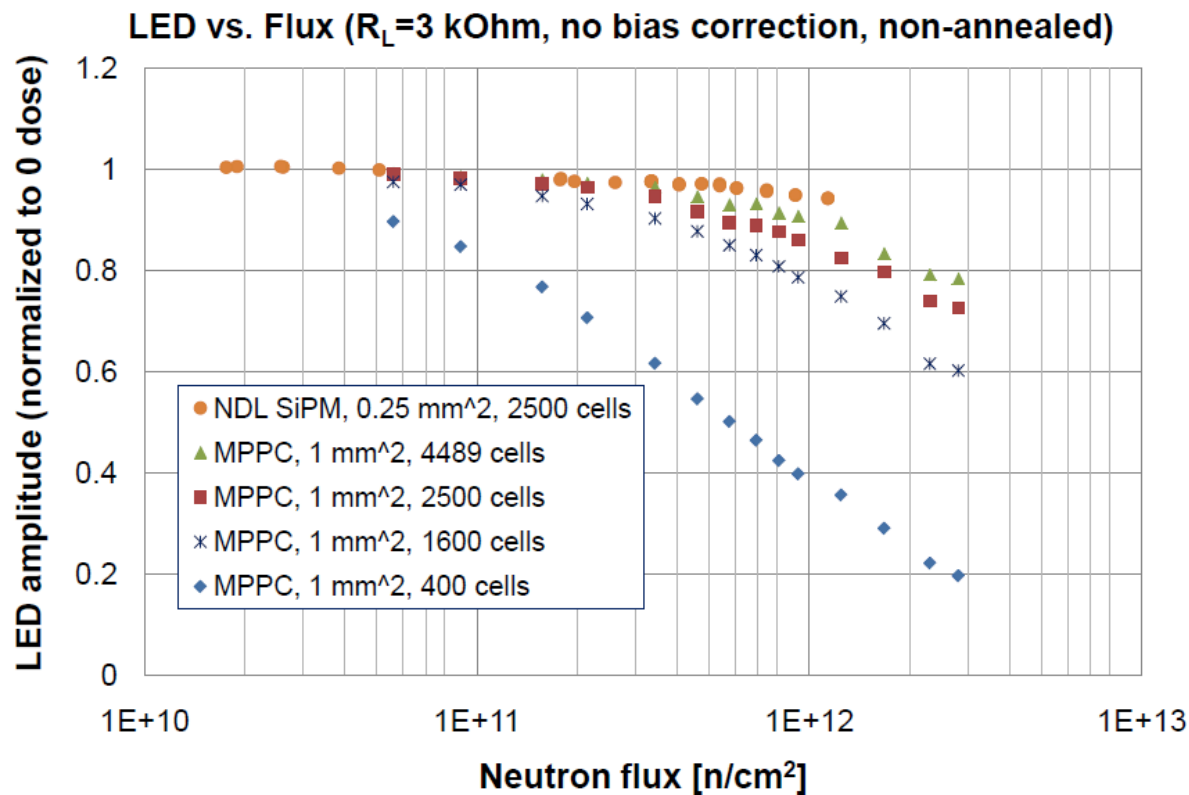
FF: fill factor

d: effective thickness

For a fixed S SiPM with more cell (smaller FF) have better radiation hardness.

Radiation hardness (II)

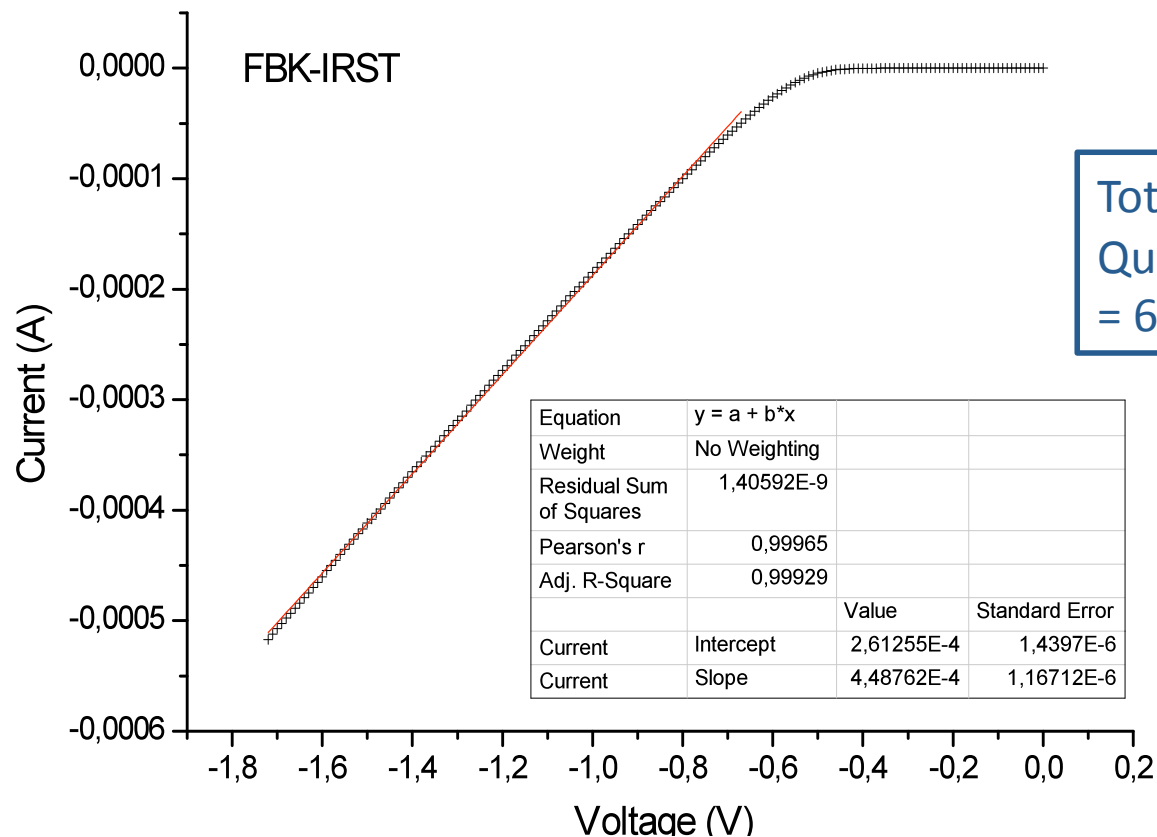
Relative response to LED pulse vs. exposure to neutrons ($E_{eq} \sim 1$ MeV) for different SiPMs



SiPMs with high cell density and fast recovery time can operate up to $3 \cdot 10^{12}$ neutrons/ cm^2 (gain change is $< 25\%$). (Musienko SiPM workshop 16-02-2011)

SiPM measurements

Forward IV: measures the quenching resistors and give a quick integrity check

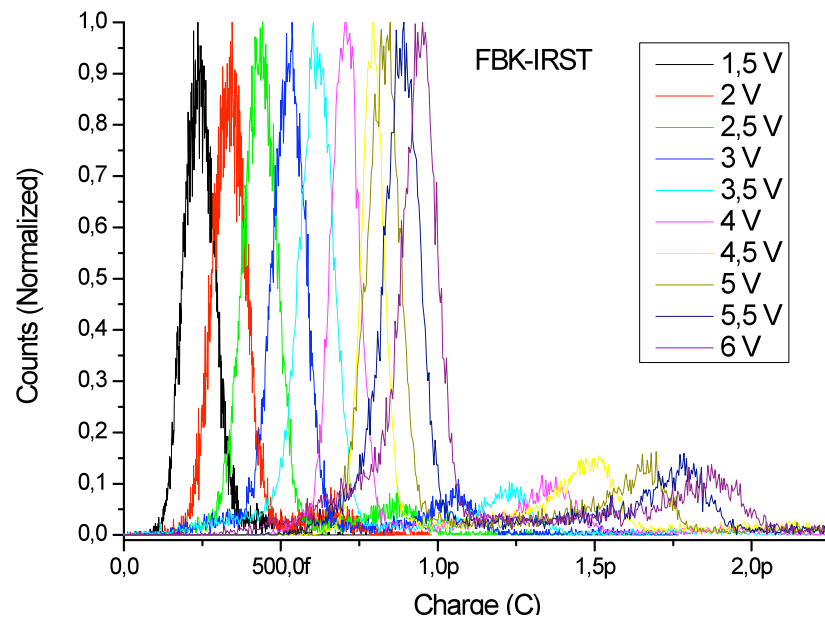


Total resistance is 2228 Ohm.
Quenching resistor is 2228×292
= 650.6 kOhm

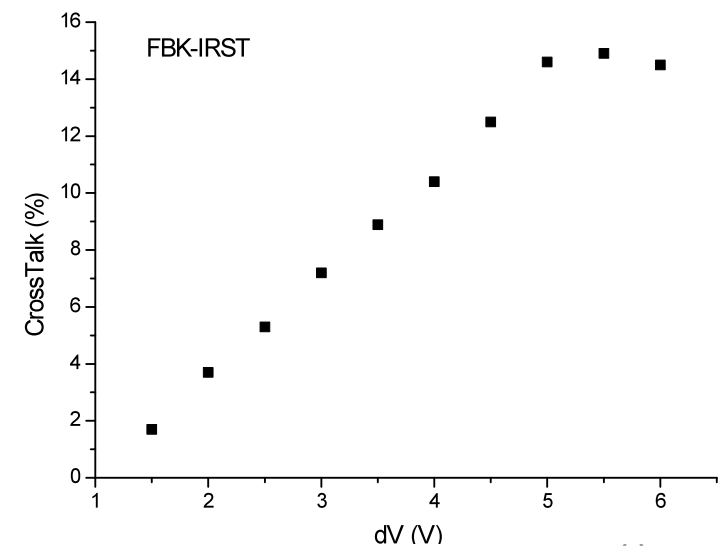
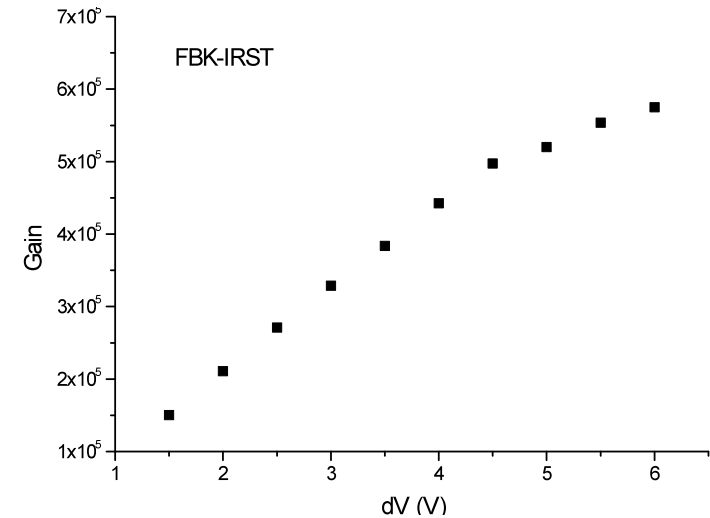
O. Starodubtsev RD11

Gain and Optical cross-talk

Charge spectrum: Integration time 5 ns.
Signal is amplified by 10



$$\text{Optical crosstalk} = N_{pe2}/N_{pe1}$$

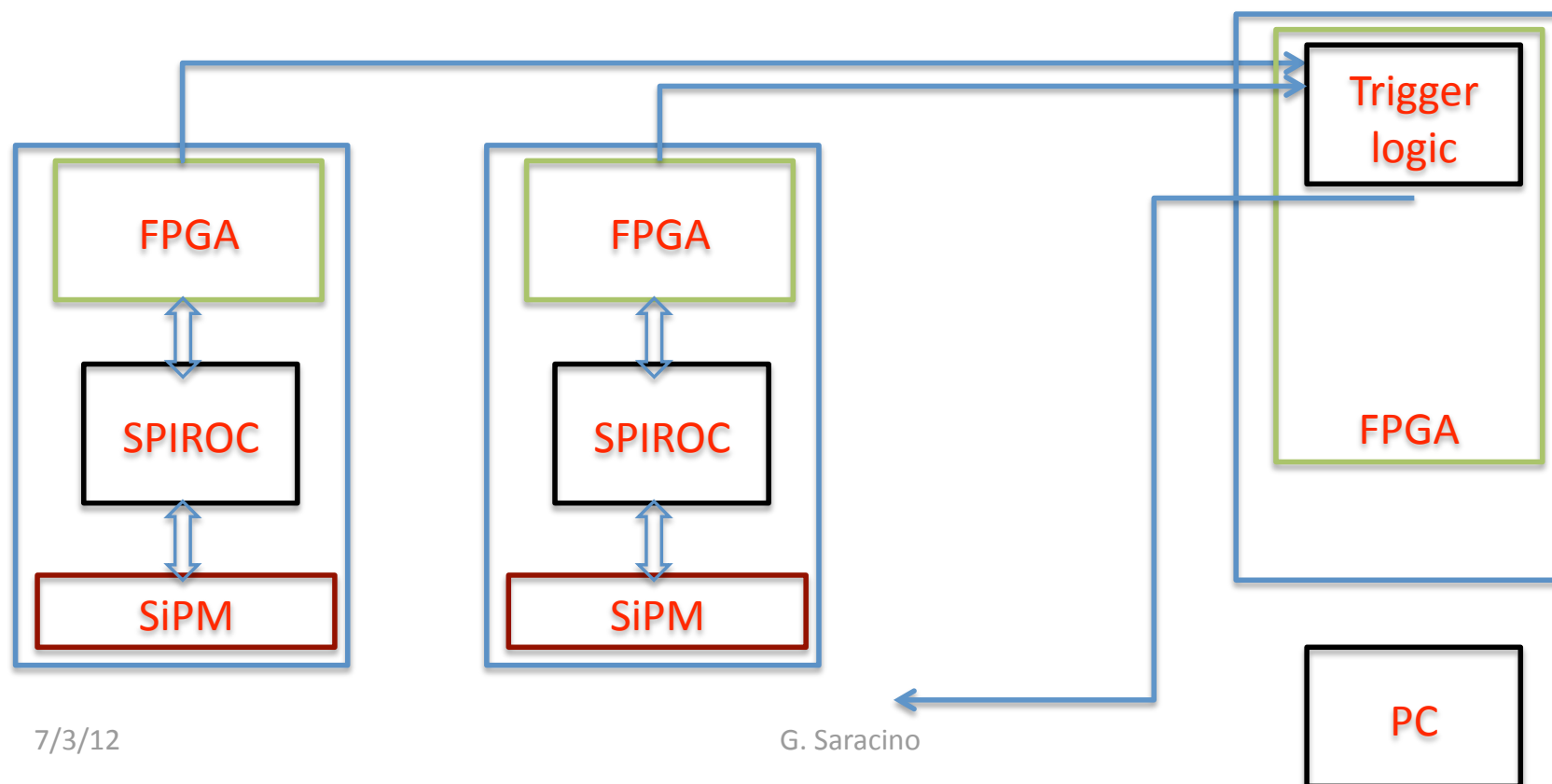


MU_RAY FEE & DAQ

The FEE board and DAQ have been designed in order to reduce power consumption.

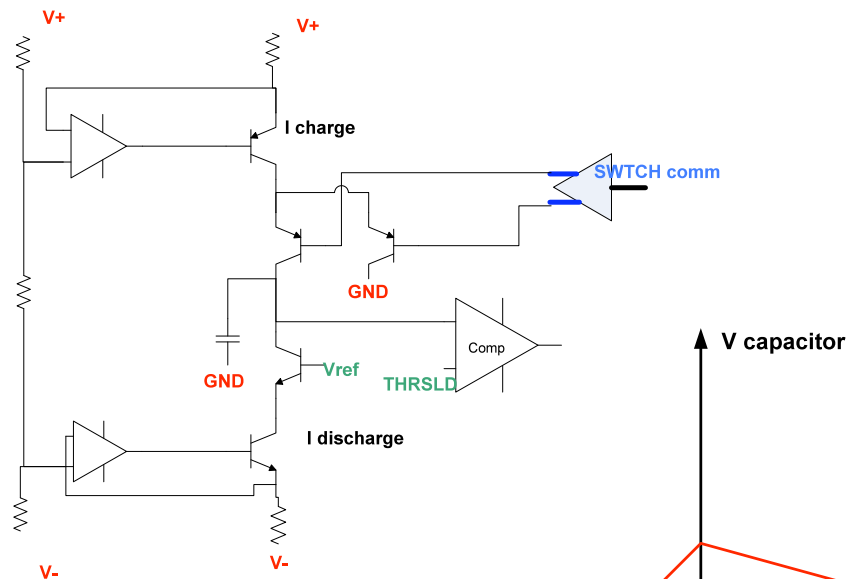
SPIROC are host in a board controlled by a FPGA (SLAVE). All the slaves are connected to a MASTER board which provides the trigger logic.

All the SLAVEs work in RUN mode, i.e. until a trigger is produced the FPGA clock is OFF and all the logic is combinatorial and power consumption is limited. When the trigger is produce, the clock is turned on and digitization and data transfer is started



MU-RAY: Time measurement

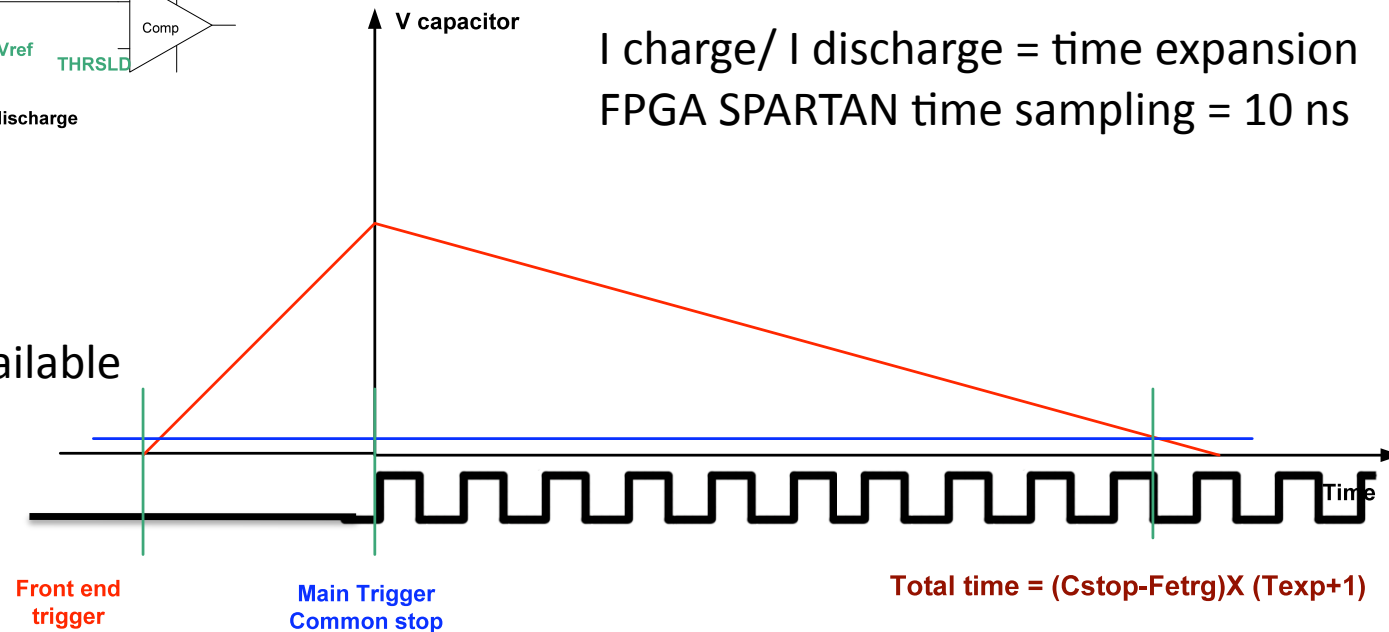
Sub-ns time resolutions can be achieved with “low” clock period using Time Expansion



We use expansion ≈ 50 and $T = 10$ ns
This allows, in principle, to ≈ 200 ps res.

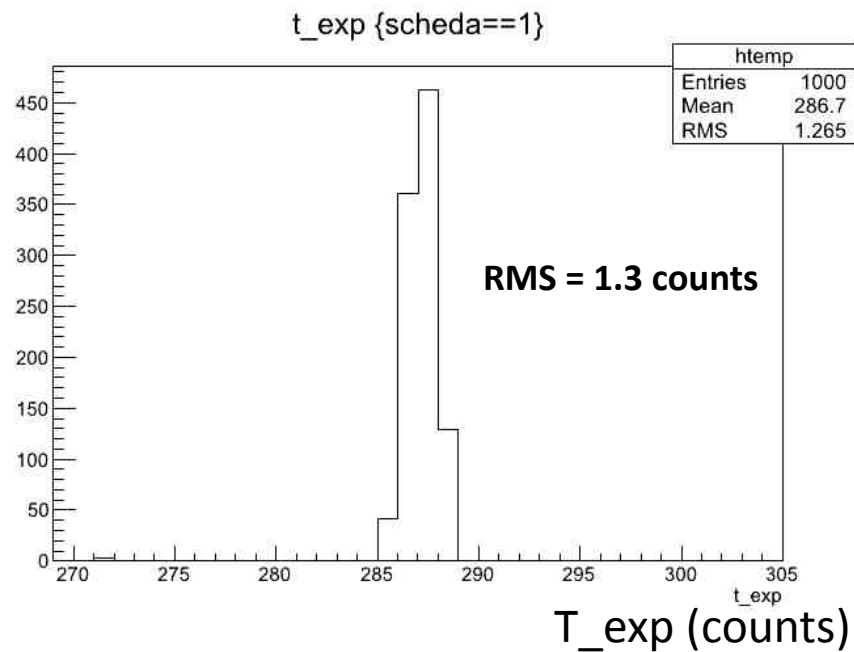
$I_{\text{charge}} / I_{\text{discharge}} = \text{time expansion}$
FPGA SPARTAN time sampling = 10 ns

No clock available
(run mode)

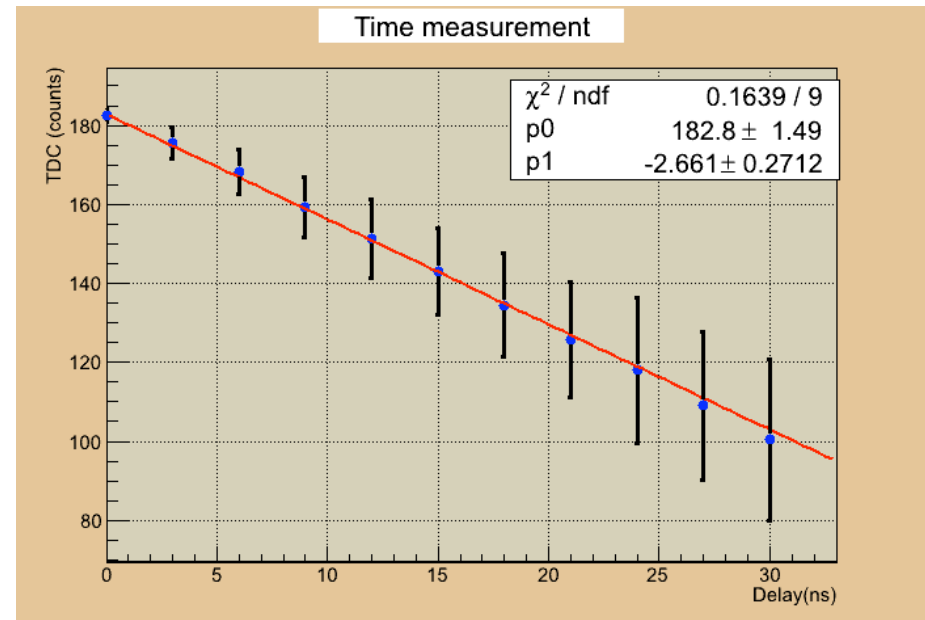


MU-RAY Time expansion

Laboratory measurements with pulse generator



Single board resolution (fixed delay)



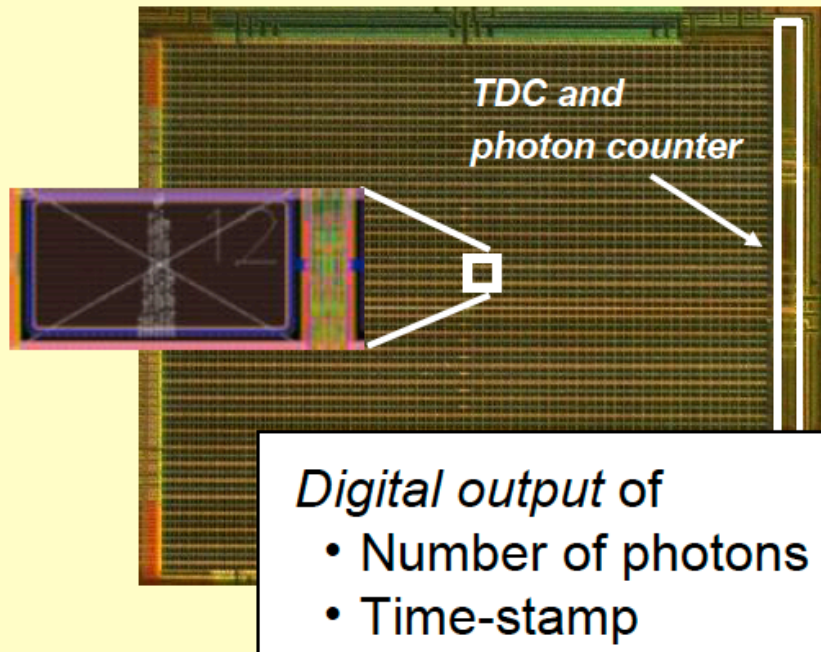
Two boards resolution (variable relative delay)

Future developments

Digital SiPM (Philips)
high density cells (hamamatsu)
low x-talk

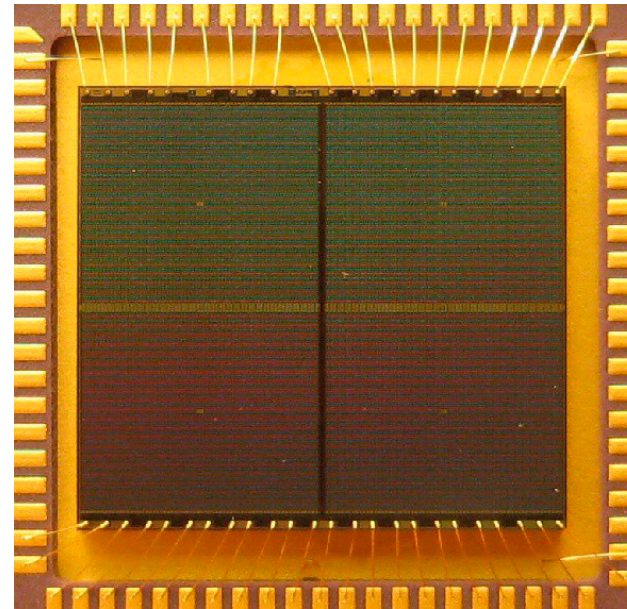
Digital SiPM

Digital SiPM



- Each diode is a digital switch
- Digital sum of detected photons
- Digital data output

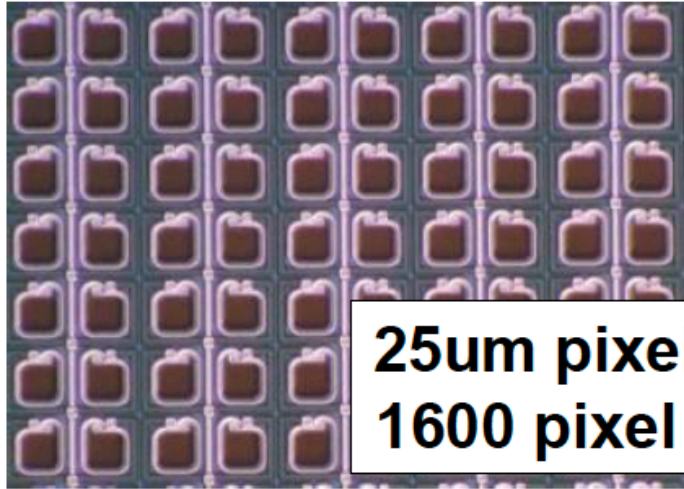
PHILIPS: DLS 6400-22 digital SiPM (2010):



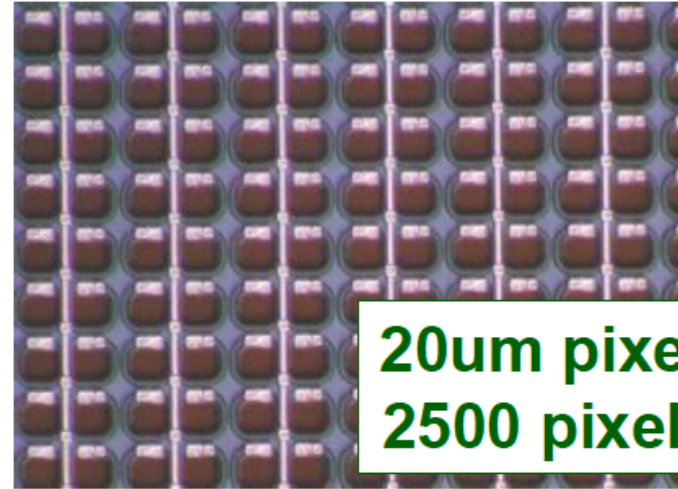
- 25600 cells
- TDCs, controller, data buffers
- JTAG for configuration & test
- 48 bond wires

Thomas Frach, LIGHT 11

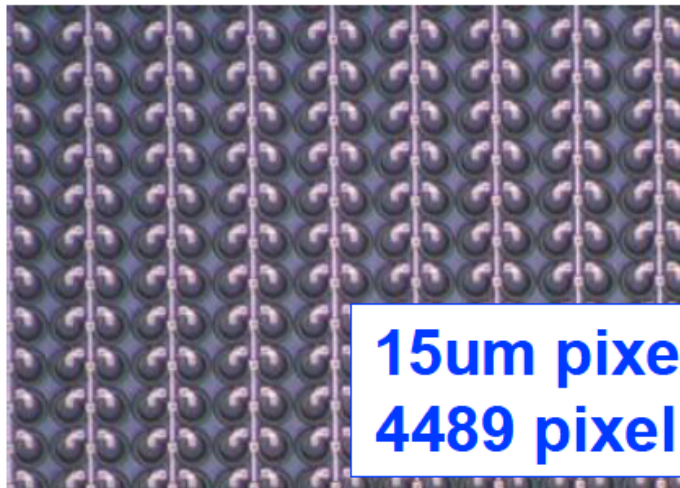
Wide dynamic range by small pixel MPPC



25um pixel pitch
1600 pixel / mm²



20um pixel pitch
2500 pixel / mm²



15um pixel pitch
4489 pixel / mm²

- **Wide dynamic range**
- **Short recovery time**
- **Low dM/dV**

Electric Models